

ABSTRACT

WINGATE, MARVIN JASON. Development of Claudin 2 and Claudin 4 in Embryonic and Hatched Chick Intestine. (Under the direction of Betty L. Black).

The epithelium of the vertebrate intestine is a dynamic structure, under constant renewal. The intestinal crypts represent a proliferative compartment that is monoclonal and is maintained by multiple stem cells. Epithelial cells migrate up the villus in sheets where they differentiate into enterocytes and goblet cells. A defining characteristic of the epithelial sheets are tight junctions that behave as a primary barrier to the diffusion of molecules through the paracellular pathway. This research utilized Western blotting to study the expression of two tight-junction proteins, claudin 2 and claudin 4, in duodenal epithelial cells from pre- and post-hatch chick intestine, as well as along the crypt-villus axis in hatched chicks. Claudin 2 expression was stronger at 20 days of incubation than at 18 days and had the greatest expression in epithelium from 2-day old chicks. Additionally, claudin 2 was found to decrease up the crypt-villus axis in duodenal epithelium from 2-day old chicks. The crypt-to-villus-tip gradient of claudin 2 is present by 20 days of embryonic development at the onset of crypt formation. The localization of claudin 2 in the crypts at 20 days may establish the adult pattern of tight junctions and prepare the intestine for the absorptive functions required soon after hatching. Conversely, claudin 4 was not detected in late embryonic or early post-hatch duodenal epithelium. Claudin 4 was expressed in the intestinal epithelium of 3-week old chickens; its expression may be dependent on feeding or other physiological factors that occur after the second day post-hatch.

Development of Claudin 2 and Claudin 4 in Embryonic and Hatched Chick Intestine.

by
Marvin Jason Wingate

A thesis submitted to the Graduate Faculty of
North Carolina State University
In partial fulfillment of the
Requirements for the degree of
Master of Science

Zoology

Raleigh, North Carolina

2008

APPROVED BY:

Betty L. Black
Committee Chair

Brenda J. Grubb

James N. Petite

DEDICATION

I would like to dedicate the work to my parents Marvin and Sharon Wingate for their love and support throughout my life and during my education. My parents always put made my health and well being their main priority, especially during my battle with childhood leukemia. This work is in the memory of my grandparents Paul and Emma Wingate and Alice Goins and in honor of my grandfather Paul Goins. Furthermore, this work is in the memory of my uncles Steve Goins, Randall Goins, and James Ray Wingate and my cousin Paul Curtis Wingate Jr.

I would like to dedicate this work to the doctors, nurses, and technicians at the West Virginia University Medical Center and Children's Hospital who cared for me and watched over my health during my sickness. I must also thank Dr. Asma Safder my local pediatrician who cared for me and referred me to WVU for treatments. This work is in the memory of my many friends who lost their battles with cancer while I was receiving cancer treatments. I must also thank the ministers and members of Bluewell United Methodist Church and my community for their thoughts and prayers during my battle with cancer.

Further dedication goes to the United Methodist Student Foundation at Radford University for the guidance and support it provided to me during my undergraduate career. I would like to dedicate this work in the memory of the former director of the foundation and great friend and mentor Carol Dunsmore. Furthermore, I would like to thank Martee Buchanan, the director of the foundation who is another great friend and mentor. She had a great hand in guiding me and helping me grow as person and friend during my time in Virginia.

BIOGRAPHY

Marvin Jason Wingate was born in Bluefield, West Virginia in 1981. He graduated both his high school and vocational nursing programs with honors. Afterwards, he attended Radford University in Radford, Virginia where he earned a bachelors degree in biology graduating Cum Laude in 2003. During his time at Radford University, Jason had the opportunity to research the developing intestine and goblet cell differentiation under the direction of Dr. James Orion Rogers. Jason then decided to pursue his interests in developmental biology and the intestine under the direction of Dr. Betty Black at North Carolina State University. Jason is an avid martial artist and practitioner of Brazilian Jiu Jitsu.

ACKNOWLEDGMENTS

I would like to acknowledge the chair of my committee Dr. Betty L. Black whose support and guidance on this project have been invaluable. She has been a great mentor as well as hands on teacher, on many occasions she assisted with my laboratory work whether it was early in my career making solutions, to culturing embryonic tissues, and isolating epithelial cells, even giving up portions of her weekend to help with my experiments. I would also like to acknowledge Dr. Brenda J. Grubb whose guidance and technical advice was also inestimable on this project. Dr. Grubb is an excellent teacher with analogies that simplify difficult concepts in developmental biology. Furthermore, I would like to thank my third committee member Dr. Jim Petite whose cell culture course added to my knowledge of scientific technique. I would also like to thank my friends and lab mates Ozkan Ozden and Bo Zhang for their support during this project. Several other people in the department deserve accolades as well including my friends William “Miller” Johnstone, Will Fields, Ben Reading, Matt Picha, Christina Nelson-Strom, as well as other members of the Borski lab. Christina’s guidance in teaching me western blotting and how to use the Odyssey scanner was extremely valuable. Special thanks also go out to Russell Borski for letting me use his lab equipment and providing me with ERK antibody and other western blotting supplies. I would also like to thank friend from Biological Agricultural Engineering Deepak Keshwani for all of his advice and support during my time at NC State. I must thank the professors who supervised my teaching assistantships: Dr. Betty Black, Dr. Bill Grant, Marta Klesath, and Dr. Mary Ann Niedzlek-Feaver. Lastly, I must thank the Zoology department staff Susan Marschalk, Linda Rudd, Chris Smith, Walt Crumpler, and Meredith Henry.

TABLE OF CONTENTS

List of Figures.....	vii
Section I. Introduction and Literature Review	1
Introduction.....	1
Justification of Embryonic Chick Intestine as a Model.....	1
Development of the Early Chick Intestine	2
Morphogenesis of the Embryonic Villi.....	4
Differentiation of Chick Enterocytes	7
Interactions of Hormones and Calcium in Epithelial Differentiation of the Chick Intestine	11
Intestinal Stem Cells	16
Canocal Wnt Signaling Pathway	18
Notch Signaling Pathway.....	19
Bone Morphogenic Protein (BMP) Signaling.....	21
Tight Junctions and the Claudin Family of Proteins.....	22
Claudin 16.....	26
Calcium and Tight Junctions	28
Development of Tight Junctions in the Chick Intestine.....	31
The Expression Pattern of Claudins 3, 5, and 16 in the One Day Old Chick Intestine.....	32
The Development of Claudins 3, 5, and 16 in the Embryonic Chick Intestine	34
Claudin Localization and Development in the Mammalian Gastrointestinal Tract	35

Section II. Materials and Methods	37
Isolation of Epithelial Cells from Intestinal Villi	37
Western Blotting	38
Section III. Results.....	41
Section IV. Discussion.....	45
Section V. Literature Cited	71

LIST OF FIGURES

Figure 1. Proposed mechanism for the maintenance and renewal of the crypt-villus axis	53
Figure 2. Claudin 2 in rat kidney and intestinal epithelium of adult chicken.....	54
Figure 3. ERK 1 expression in embryonic duodenal epithelium at days 18 of development.....	55
Figure 4. Claudin 2 Expression in embryonic duodenal epithelium at 18 days of development.....	56
Figure 5. ERK 1 expression in embryonic duodenal epithelium at 20 days of development.....	57
Figure 6. Claudin 2 expression in embryonic duodenal epithelium at 20 days of development.....	58
Figure 7. ERK 1 expression in duodenal epithelium from pre- and post-hatch chicks	59
Figure 8. Claudin 2 expression in duodenal epithelium from pre- and post-hatch chicks.	60
Figure 9. ERK 1 expression in duodenal epithelium along the crypt-villus axis of the 2- day post-hatch chicks.....	61
Figure 10. Claudin 2 expression in duodenal epithelium along the crypt-villus axis of the 2- day post-hatch chicks.....	62
Figure 11. ERK 1 expression in duodenal epithelium along the crypt-villus axis of 20- day embryos.....	63
Figure 12. Claudin 2 expression in duodenal epithelium along the crypt-villus axis of the 20 day embryos.....	64
Figure 13. Claudin 4 expression in duodenal epithelium from pre- and post-hatch chicks	65
Figure 14. Claudin 4 expression in duodenal epithelium along the crypt-villus axis of 2-day chicks	66
Figure 15. Claudin 4 expression in duodenal epithelium of a 3-week old chicken	67

Figure 16. ERK 1 expression in duodenal epithelium from a 3-week old chicken 68

Figure 17. Claudin 2 expression in duodenal epithelium of a 3-week old chicken 69

Section I. Introduction and Literature Review

Introduction

Claudin proteins are a component of epithelial tight junctions in vertebrate animals. There are many types of claudin proteins and they show varying expression patterns depending on the organ in which they are located. The expression patterns of claudin 2 and claudin 4 have not been examined in embryonic chick intestine or along the crypt-villus axis of hatched chicks. The goal of the present study is to examine the development of claudin 2 and claudin 4 in epithelial cells from embryonic chick intestine and along the crypt-villus axis of young chicks by using Western blotting technique.

Claudin 2 and Claudin 4 have opposing functions in epithelia. Claudin 2 is associated with “leaky” tight junctions where it acts as a cation pore (VanItallie et al. 2003), whereas claudin 4 is a “sealing” claudin which decreases the paracellular permeability through tight junctions. These claudins were chosen for the present study because they have different properties and opposite functions (See Review by Krause, 2007). The hypothesis of the study is that claudins 2 and 4 will have different expression patterns during development and along the crypt-villus axis, with claudin 2 becoming localized within the crypts and claudin 4 on the villi as the intestinal epithelium matures.

Justification of Embryonic Chick Intestine as a Model

The small intestine of embryonic chicks serves as an excellent model for the study of intestinal development and differentiation. Fertile eggs are readily available and can be

obtained and maintained cheaply. The developing embryo is free from circulating maternal hormones and signaling. The morphogenesis of the embryonic chick is well understood and documented (Hamburg and Hamilton, 1951), as is morphogenesis of the embryonic intestine (Hilton, 1902; Coulumbre and Coulumbre 1952; Grey, 1972). Developing intestine can be maintained in defined culture medium (Black, 1977).

Development of the Embryonic Chick Intestine

The small intestine of the embryonic chick arises from splanchnopleure, which is composed of splanchnic mesoderm and endoderm. The endoderm forms the epithelium and the splanchnic mesoderm forms the muscle layers and mesenteries.

In the late 1950's Coulumbre and Coulumbre examined the role of mechanical factors in the morphogenesis of the embryonic chick duodena (Coulumbre and Coulumbre, 1958). Coulumbre and Coulumbre determined that the length and diameter of the embryonic chick intestine increases in altering stages. Two stages of rapid lengthening can be observed in the embryonic duodena; the first occurs between the eighth and fourteenth day of development. The second stage occurs after the twentieth day of development. An increase in duodenal diameter occurs between the fourteenth and twentieth days of development (Coulumbre and Coulumbre, 1958).

A study by Hinni and Watterson conflicted with some of the findings of Coulumbre and Coulumbre (Hinni and Watterson, 1963). Conflicts with duodenal lengths include the following. First, values are smaller by 6-10 mm by 16 and 20 days of development and as much as 16 to 23 mm at days 21 and 22, respectively. Secondly,

plateaus observed between 15 and 18 days aren't as evident; however, Hinni and Watterson reported growth is slowed during this period. Finally, the cessation of growth isn't as prevalent as previously reported by Coulumbre and Coulumbre. Differences in bird breeds may be one cause of discrepancy. Hinni and Watterson utilized the white leghorn strain while Coulumbre and Coulumbre used chicks from the Cornish-Rock cross variety. Secondly, methods differed between the two lab groups. Coulumbre and Coulumbre used lived tissue soaked in blood, while Hinni and Watterson used tissue that had been preserved in 100% cold alcohol (Hinni and Watterson, 1963).

Coulumbre and Coulumbre also examined the differentiation of the mesenchyme and muscles layers of the developing intestine (Coulumbre and Coulumbre, 1958). At the fourth day of development the epithelium of the duodena is pseudo-stratified columnar epithelium surrounded by mesenchyme and the external serosa. From the fourth day to the eight day the epithelial layer increases in area by cell division, and the surrounding mesenchyme becomes circularly oriented. Around the eighth day circularly oriented smooth muscle has differentiated. After eight days of incubation the mesenchyme on either side of the circular muscle has become oriented longitudinally. At approximately 12 or 13 days of incubation the mesenchyme on either side of the circular muscle differentiates into longitudinal muscle, with the innermost layer becoming the muscularis mucosae, and the outer most layers becoming the longitudinal smooth muscle layer (Coulumbre and Coulumbre, 1958).

Morphogenesis of the Embryonic Villi

In the early 1900's, Hilton described the changes in form of the mucosal topography. In embryonic chick intestine villi aren't directly formed, rather longitudinal foldings called previllous ridges are the structures from which villi develop (Hilton, 1902). This suggested that mechanical factors are important in the morphogenesis of the embryonic intestine (Hilton, 1902).

Until approximately 6 days of development the lumen of the embryonic intestine is smooth, and the epithelial layer is psuedostratified (Coulombre and Coulombre, 1958; Grey 1972). On the seventh or eighth day of development two longitudinal ridges appear, named the first rank of previllous ridges (Coulombre and Coulombre, 1958). From the eight day of development to the twelfth day of development there is a mathematical progression in ridge number. On the ninth or tenth day of development the second rank of previllous ridges form in-between the first rank of previllous ridges (Grey, 1972). On the tenth or eleventh day of development four new ridges appear which forms the third rank of previllous ridges (Grey, 1972). At the twelfth day of development the previllous ridges form a zig-zag pattern (Coulombre and Coulombre, 1958). On the thirteenth day of development eight more previllous ridges arise, forming the fourth rank of previllous ridges (Grey, 1972). At sixteen days of development the previllous ridges become indented and the fifth rank of previllous ridges begins forming (Coulombre and Coulombre, 1958; Grey, 1972).

Scanning electron microscopy reveals three major events in the development of the first four previllous ridges (Grey, 1972). These events are as follows; first, elevation

of the previllous ridges; secondly, delineation of the villus base; finally, outgrowth of definitive villi occur (Grey, 1972). By day 17 the true villus formation can be seen (Grey, 1972). At the eighteenth or nineteenth day of development the first four ranks of villi elongate rapidly and the zig-zag pattern is obscured (Coulombre and Coulombre, 1958; Grey, 1972). By the nineteenth day of development the adult pattern of villi can be observed in the embryonic duodena (Coulombre and Coulombre, 1958). By the eighteenth or nineteenth day the fifth rank of villi grow rapidly (Grey, 1972). During the nineteenth or twentieth day the fifth rank of villi develop bulb like swellings (Grey, 1972). On the twentieth day of development the fifth rank of villi begin to resemble the pattern observed in other villi. At four days post-hatch the fifth rank of villi can't be distinguished from the other ranks of villi (Grey, 1972).

Coulombre and Coulombre concluded that the appearance and contraction of the first smooth muscle layer on the eighth day of development is important for two reasons. First, radial compression caused by the contracting muscle and mucosal epithelium form the first two folds, which are the first and second rank of previllous ridges. This events set up the mathematic progression of previllous increase. Secondly, the contracting muscle layer limits the radius of the duodena. This restriction in radius causes a period of duodenal lengthening. This elongation may initiate the mesenchyme on either side of the circular muscle to differentiate into the muscularis mucosae and longitudinal muscle, respectively (Coulombre and Coulombre, 1958).

A study by Burgess examined the events prior to previllous ridge formation and provides more insight into the mechanisms of ridge formation (Burgess, 1975). At 4.5

days of incubation the embryonic intestinal epithelium appears in cross-section as a thick walled tube with a small lumen. Cross sections from 5-7 day old embryos reveal an elliptical epithelium with an expanding lumen. The circumference of the ellipse increases from 7-8 days. At approximately 8 to 8.5 days of incubation the elliptical tube forms a triangular shaped tube. From the triangular shaped tube three ridges form as the epithelium folds toward the lumen. The second ranks form in-between the valley occupied by the first rank of previllous ridges, bringing the total number of previllous ridges to six (Burgess, 1975). This number conflicts with Coulumbre and Coulumbre previous findings; however Burgess used a different region of the duodenum.

Burgess then tested the hypothesis that the formation of smooth muscle provides mechanical pressure to initiate ridge formation (Burgess, 1975). The mesenchyme from one side of the elongated elliptical stage of intestine (eight days incubation) was removed. This experiment prevented the smooth muscle from being continuous, thus preventing it from exerting force onto the epithelial layer. After culturing the tissue ridge formation occurred as normal and the smooth muscle was replaced with mesenchymal tissue. Splitting the duodenum lengthwise and culturing it didn't inhibit ridge formation; however it was delayed by approximately 24 hours. Burgess found that mesenchyme was required for ridge formation as isolated epithelial tubes don't form ridges.

Burgess then exposed cultured tissue to Cytochalasin-B; which inhibits cellular movements and disrupts microfilaments (Burgess, 1975). Culture of eight day old intestine in 1ug/ml Cytochalasin-B prevented ridge formation and caused the apical surface of the cells to bulge into the lumen. The apical cytoplasm of these cells contained

many granules in place of normal microfilaments. Burgess concluded that neither muscle layer motility nor mitotic pressure causes ridge formation, but cytoplasmic microfilaments are responsible for folding (Burgess, 1975).

Differentiation of Chick Enterocytes

In the late 1950's Moog and Thomas measured the accumulation and loss of glycogen in embryonic chick duodena and the influence of hydrocortisone acetate on glycogen levels (Moog and Thomas, 1957). Glycogen is maximal in the duodenum of embryonic chicks at 18 days and then rapidly decreases. The accumulation of glycogen begins steadily at 14 days and then intensifies between 14 and 16 days of incubation. The physiologically active soluble form of glycogen and the insoluble form of glycogen were examined; most of the glycogen present was the physiologically active form.

Injection with the hormone hydrocortisone acetate (HCA) accelerates the accumulation of glycogen levels in the embryonic duodenum. Injection of HCA at 14 days accelerates the levels of 17 day glycogen levels to those of a 18 or 19 day old embryo. When a 14 day old embryo is injected with HCA maximal glycogen levels are reached at 16 days as opposed to 18 days. Following injections with HCA, glycogen levels were significantly greater than the *in vivo* levels of an 18 day old embryo when comparing a treated embryo at 16 days. When embryos of 16, 17, or 18 days are treated with HCA the accumulation of glycogen is enhanced but the subsequent loss of glycogen is also enhanced. Interestingly, when an 18 day embryonic duodena is treated with HCA, glycogen levels don't exceed control values at 18 days, but treated groups maintain

higher glycogen levels. Moog suggested that the fall in glycogen after 18 days in the embryo may supply micronutrients to support further differentiation and cellular processes. She also suggested that HCA speeds up development without dissociating other mechanisms. Finally, she suggested that HCA can increase both phosphatase and glycogen levels in the embryo (Moog and Thomas, 1957).

The three days prior to hatching are marked by dramatic morphological and function changes in the chick intestine. Enterocytes are increasing in height while their microvilli increase in both height and density the days prior to hatching (Black, 1976, 1978). Prior to hatching, metabolism increases epithelial glycogen and lipid stores are depleted possibly to provide energy for proliferation and differentiation. Glucose active transport is present in 12 day old embryos and then increases by 11 fold the four days after hatching (Black, 1988). In uncultured duodena from broiler strain embryos alkaline phosphatase activity increases approximately four fold between days 14 and 17 (Black, 1988). Sucrase activity increases almost 2 fold between day 14 and 17. Glycogen content of the duodenal epithelium almost doubles from day 14 to 17 in broiler strain chicks.

Black examined the influence of 1nM thyroxine (T_4) and 1 μ M Hydrocortisone (HC) glucose and glycogen metabolism in culture. When 14 day old embryonic duodena is cultured in the presence of 1nM T_4 glycogen levels drop below those found at the beginning of culture (Black, 1988). Conversely, when 1 μ M HC is added to the culture medium the duodena accumulate 145% of the paired control's glycogen values.

Black also examined glycogen turn over rate using (^{14}C) glucose incorporation into the tissue (Black, 1988). Tissues cultured with 1nM T_4 for 72 hours contained

significantly less labeled glycogen than the paired controls. The opposite effect was observed with 1 μ M HC the treated group contained 135% of the control cultures labeled glycogen values. The ability of embryonic chick intestine to oxidize glucose into CO₂ was measured throughout the third week of development. Glucose oxidation decreases from embryonic days 14 to 18 *in vivo*, and then rises rapidly between days 19 and 21. The addition of 1nM T₄ to the culture media elevates glucose oxidation while 1 μ M HC depresses glucose oxidation. Black suggested that circulation HC may regulate the embryonic intestine during days 14-18 when metabolism is slow and glycogen levels are accumulating. Conversely, Black suggests T₄ regulates the utilization of glycogen for energy and the functional differentiation as the chick prepares to hatch (Black, 1988).

Black and Moog examined the influence of hydrocortisone and thyroxine on alkaline phosphatase and maltase activity in the embryonic chick intestine (Black and Moog, 1978). When 14 day embryonic duodena are cultured for 48 hours in media containing 5 X 10⁻⁷ to 1 X 10⁻⁶ M hydrocortisone, alkaline phosphatase activity is increased 38% above the unsupplemented medium. Hydrocortisone ranging from 5 X 10⁻⁸ to 1 X 10⁻⁵ M increased maltase activity 42% above the unsupplemented media. When 16 day embryonic duodena are cultured with hydrocortisone, alkaline phosphates levels rise 10% to 62% depending on hormone concentration with the optimum increase in activity 5 X 10⁻⁶ M hydrocortisone. Maltase activity rose 29% above unsupplemented medium when cultured with 2 X 10⁻⁶ M hydrocortisone. When tissue from 12 to 18 day old embryos is cultured with thyroxone (T₄) alkaline phosphatase levels are elevated at all stages except 18 days with a concentration of 10⁻¹⁰M T₄. A large amount of activity

was also seen in the culture media. A similar trend was seen when maltase was examined; increases were seen in all stages except 18 days, with a large amount of activity in the culture medium.

(Black and Moog 1978) then examined the effect of culturing the tissue with or without T4 on alkaline phosphatase activity and compared those values to the untreated duodenum at the appropriate ages. When 12 or 14 day duodena are cultured in unsupplemented medium, alkaline phosphatase activity increases by two fold when compared to untreated explanted tissues. With the addition of 10^{-8} M T4 even greater alkaline phosphatase activities can be seen when compared to the 12 and 14 day untreated explants. Hormone-free medium didn't increase maltase activity above the *in ovo* levels.

In *in ovo* embryos alkaline phosphatase levels are low in the intestine and absent from the luminal surface of the epithelium from 10 to 16 day (Moog, 1950). Increases are observed in alkaline phosphatase activities at 16 days of incubation. Maltase activities are also low at 14 days and rise steadily thereafter. Culture with 10^{-6} M hydrocortisone is able to maintain levels of maltase relative to the intact embryo for 72 hours (Black and Moog, 1978). Culture with 10^{-8} T4 increases maltase activity after one day, reaches a maximum at three days, and then proceeds to decline. Culture with either hydrocortisone or T4 causes significant maltase activity to be released in the culture medium. T4 and hydrocortisone were also looked at in combination in culture and both hormones provided additive increases in activity of both enzymes. Black and Moog concluded that both thyroid and glucocorticoid hormones play an important role in the differentiation and maturation of the intestine (Black and Moog, 1978).

Interactions of Hormones and Calcium in Epithelial Differentiation of the Chick

Intestine

In the early 1960s Hinni and Watterson examined the effect of hormones on intestinal development by removing the pituitary of developing chicks (hyposectomy) (Hinni and Watterson 1963). Hinni and Watterson determined that goblet cell differentiation is altered in four ways in the absence of pituitary hormones. First, the numbers of goblet cell primordia are less. Secondly, goblet cell primordia migrate to the apices of villi more slowly. Thirdly, this goblet cell population fails to produce normal amounts of mucin, as determined by alcian blue staining. Lastly, the goblet cells fail to exocytose their mucin contents into the lumen (Hinni and Watterson 1963).

In the duodena of embryonic chicks, *in vivo*, goblet cell numbers are as follows; 10 per 100 ridges at 14 days, 236 per 100 ridges at 18 days, and 596 per 100 ridges at 19 days (Black, 1977). Culturing embryonic chick in defined media (medium 199) significantly increased goblet cell numbers when compared to *in vivo* duodena. Furthermore, the addition of 10^{-9} M thyroxone increased goblet cell numbers when compared to control tissues. The addition of 10^{-6} M hydrocortisone inhibited goblet cell differentiation. Black suggested that hydrocortisone may act as a circulating inhibitor of differentiation during the third week on development in embryonic chick intestine (Black, 1977).

Later Black's lab examined whether calcium has a role in the modulation of goblet cell differentiation. The calcium ion concentration in media 199 is higher than the

calcium ion concentration required to initiate differentiation in other tissues (Black and Smith, 1989). When 14 day old embryonic chick duodena is cultured in media containing calcium concentrations from 0.9-2.0mM for 48 hours, goblet cell differentiation is altered. As the calcium concentration in culture was increased from 0.9-2.0mM, goblet cell counts increased from 29 per 100 ridges to 158 per 100 ridges. Culture media of 1.6mM calcium produced maximum goblet cell differentiation; this calcium level is equivalent to the serum calcium of an 18 day old chick embryo. It was concluded that during the last week of embryonic development, calcium in concert with circulating hormones mediates goblet cell differentiation (Black and Smith, 1989).

Black and Rogers later examined the calcium homeostasis in the embryonic and neonatal intestine (Black and Rogers, 1992). Using Fura-2 assays the cytoplasmic calcium concentration of duodenal cells throughout development was examined. Cytoplasmic calcium concentrations in intestinal epithelium of developing embryo is follows; 76-80nM in 14-17 day old intestine, levels increase 20% in 17-19 day old embryos to 92-98nm, calcium levels increase approximately 130% in 20-1day old post-hatch neonates to 209nm, and finally, calcium levels in adult tissue drop to 133-142nm, which is 70-80% higher than early embryonic levels of calcium. Black and Rogers speculated that the higher post-hatch level of calcium may be required to initiate/maintain cellular differentiation. No significant cytoplasmic calcium gradient exists along the embryonic villus (from base to tip). Alkaline phosphatase activity, which is a marker of enterocyte differentiation, was correlated to cytoplasmic calcium concentration. Both parameters are low during embryonic day 14 and increase at embryonic day 17 and

during hatching. This suggests that cytoplasmic calcium along with hormones regulates the ontogeny of some enterocyte enzymes and the differentiation of goblet cells (Black and Rogers, 1992).

Black and Rogers later examined the effects of hydrocortisone and thyroxine on calcium homeostasis in developing chick duodena (Rogers and Black, 1996). When 14 day old duodena is cultured in defined medium with 1.3mM calcium over the time course of 72 hours, epithelial cytoplasmic calcium levels are significantly less than tissue of comparable ages *in vivo*. Epithelium explanted at 14 days and cultured for 48 hours is also unable to maintain low cytoplasmic calcium levels when placed in a calcium “challenge”, in which extracellular calcium levels are changed from 0.7mM to 7.0mM, respectively. In contrast, 16 day old uncultured duodenal epithelium is better able to resist the calcium “challenge”. Cultured 14 day old duodena has a 230% increase in cytoplasmic calcium, while the 16 day old uncultured tissue has an 83% increase in cytoplasmic calcium (Rogers and Black, 1996).

When 14 day old embryonic duodena is cultured in defined media (1.3mM calcium) containing HC or T4 for 72 hours, cytoplasmic calcium levels were maintained significantly higher than tissues cultured without hormones (Rogers and Black, 1996). Furthermore, after 48 hours of culture HC increased cytoplasmic calcium levels to 42% of the control values, while T4's effect wasn't significant. Cytoplasmic calcium levels became significantly higher than those of control cultures after only four hours of culture with HC and reached a maximal value after 12 hours. Lastly, Rogers and Black determined that cells from HC or T4 treated duodena cultured for 48 hours resist calcium

“challenge” better than control tissues. Black and Rogers concluded that HC has an effect on the calcium homeostasis of the developing chick epithelium. Furthermore, it was proposed that effect of HC on cytoplasmic calcium levels may be due in part to a decreased influx of calcium through the microvilli combined with a decrease in calcium efflux across the basolateral membranes, and suggest a nuclear hormone mechanism where changes in cytoplasmic calcium concentration may alter epithelial differentiation (Rogers and Black, 1996).

In 2002 Mack and Black further examined the roles of extracellular calcium on the developing chick intestine (Mack and Black, 2002). Sixteen and eighteen day old embryonic chick intestine was cultured in varying calcium concentrations. Alkaline phosphatase levels in 16 day old duodena cultured in low calcium 0.7mM were unchanged after 48 hours. The ALP levels in 18 day old tissue cultured in low calcium were decreased by 30%, but not significantly. Conversely, ALP values of 16 and 18 day old tissue cultured in high calcium (2.8mM) were 244 and 206% greater, when compared to low calcium cultures. Next, the influence of calcium homeostasis disruptors and calcium channel blockers on ALP levels were investigated. When 16 and 18 day old tissue was cultured in media containing lead acetate ALP levels were decreased. The ALP levels of 18 day old tissue cultured in media containing lead were decreased below normal baseline values. This indicated that lead, a calcium antagonist, reversed the accelerated differentiation normally seen in this lab’s culture system.

When 16 day old tissue is cultured in media containing verapamil, ALP levels are increased. However, when 18 day old tissue is cultured with verapamil ALP levels are

decreased by 53%. Nifedipine an L-type calcium channel blocker reduces ALP levels in both 16 and 18 day old cultured tissue. These results suggested that extracellular calcium may influence enterocyte differentiation via voltage specific calcium channels.

Black and Mack also examined the role of extracellular calcium on goblet cell differentiation. When 16 and 18 day old tissue embryonic tissue is cultured in control media 199 significant increases in goblet cell differentiation are observed when compared to uncultured baseline values. Goblet cell numbers increased in a dose dependant manner when calcium concentrations were increased from 0.7mM to 2.8mM calcium. This trend is similar to that observed by Black and Smith who cultured 14 day old tissue in varying calcium concentrations (Black and Smith, 1989). Furthermore, goblet cell differentiation was inhibited by lead acetate in both 16 and 18 day old cultured tissues, reaching only 35 and 48% of the paired controls, respectively. In a manner similar to its effects on ALP, verapamil only inhibited differentiation in 18 day old tissue, while nefidipine lowered goblet cell numbers in both 16 day old and 18 day old cultured tissue. These findings suggested a mechanism in which calcium antagonists inhibit goblet cell differentiation by preventing the influx of extracellular calcium across the plasma membrane (Mack and Black, 2002).

Mack and Black examined cytoplasmic calcium levels via the fluorescent probe Indo-1 (AM) and confocal microscopy. Mack and Black noted clear epithelial layer calcium signaling in 19 day old uncultured tissue. Eighteen day old tissue cultured for 24 hours displayed greater fluorescence than the uncultured tissue, especially in the apical microvillar region with the most fluorescence located at the basal regions. Tissues

cultured in verapamil or nifedipine exhibited a lesser and more uniform fluorescence when compared to the controls. A reduction in calcium fluorescence was especially noted in the apical brush border region of the treated tissue. The reduction of fluorescence in the apical brush border correlates with the idea that brush border calcium levels alter ALP activity. The differences in fluorescence were quantified and revealed that both treatment groups significantly lower brush border calcium levels as well as cytoplasmic calcium levels, respectively. It is interesting to note that while both brush border and cytoplasmic calcium levels were reduced in the treatment groups; the ratio of brush border to cytoplasmic calcium was not significantly decreased when compared to the paired control tissue. However, it was noted that the decrease in cellular calcium could still alter normal intracellular calcium signaling cascades. This finding further supported the hypothesis that extracellular calcium alters epithelial cell differentiation via voltage sensitive calcium channels (Mack and Black, 2002).

Intestinal stem cells

The epithelium of the vertebrate intestine is a dynamic structure, under constant renewal, and the intestinal crypts represent a proliferative compartment that is monoclonal and is maintained by multiple stem cells. In an excellent review of signaling pathways of the intestine Scoville et al. define intestinal stem cells “as cells that give rise to all types of mature intestinal epithelium and at the same time replenish themselves through “self renewal”, (See Review by Scoville et al. 2008). The villi contain cells that arise from two main lineages; the secretory lineage from which enteroendocrine cells,

paneth cells and goblet cells arise and absorptive cells from which enterocytes arise

Figure 1 (See Reviews by Hauck et al. 2005, Barker et al. 2008 and Scoville et al. 2008).

Each villi is maintained by multiple crypts thus each villi is polyclonal. Two different pools of stem cells are currently thought to supply each villus. The first pool of stem cells are located in the 4th-6th position meaning this cell type is located 4 to 6 cells above the crypt base which contains paneth cells that secrete antimicrobial lysozymes. +4 cells are quiescent and cycle slowly and retain label markers for long periods of time and are termed +4 label retaining cells or +4LRCs. +4 cells express Musashi-1 which inhibits inhibitors of the Notch pathway as well as antagonists to the Wnt pathway. The second stem cell population is located in the crypt base and is interspersed with paneth cells.

Screen that examined Wnt genes up regulated in colon cancer revealed a gene located in a single cell type in the crypt base. Lgr5/GPR49 is a leucine rich orphaned uncoupled G-protein receptor that is expressed in crypt based columnar cells CBCs. This protein encodes a leucine rich receptor that is closely related to glycoprotein hormone ligands, such as TSH, FSH, and LH hormone receptors (see review by Barker et al. 2008). Lgr5+ CBCs are multipotent for all four cell types, undergo self renewal, persist for 60 days, and are resistant to irradiation (see review by Scoville et al. 2008). Scoville et al. suggest that both cell types are the intestinal stem cells because recent findings in bone marrow provides evidence for two cell populations; one long term quiescent cell type and one active cycling cell type. The authors propose a model where the Lgr5+CBCs maintains regenerative properties under normal conditions and the +4LRS act as a backup population in case of injury (See Review by Scoville et al. 2008). Several signaling

pathways are required to maintain the intestinal stem cells, proliferating crypts, and differentiating villi these pathways include the following; Wnt, Notch, Sonic Hedgehog, Bone Morphogenic Protein, and PtdIns(3,4,5) Kinase PI3K (See Reviews by Hauck et al. 2005, Barker et al. 2008 and Scoville et al. 2008). The Wnt, Notch and Bone Morphogenic Protein signaling pathways will be briefly discussed below as they are the most relevant to this study.

Canonical Wnt Signaling Pathway

The Wnt signaling pathway is found in all metazoans. Wnts are a family of 19 secreted glycoproteins and act through the frizzled receptor in a paracrine or autocrine manner (See Reviews by Pinto and Cleavers, 2005, Hauck et al. 2005, and Scoville et al. 2008). The Wnt pathway is involved in several processes in the intestinal epithelium: maintaining the stem cell pool via cell cycle control and inhibition of differentiation, controlling the localization and migration of cells along the crypt-villus axis, and directing the secretory lineage cells as well as the terminal differentiation of paneth cells. The canonical Wnt signaling pathway, which involves the nuclear protein β -catenin is important in the maintenance of the progenitor pool; both +4LRS and Lgr5+CBCs express components of the Wnt pathway (See Reviews by Barker et al. 2008 and Scoville et al. 2008). Once Wnts bind the frizzled receptor, this activates the stabilization of the β -catenin complex. In an unstimulated state, β -catenin is bound to a destruction complex containing several proteins including the following; the scaffold protein Axin, Adenomatous Polyposis Coli (APC) a tumor suppressor gene, kinase casein kinase I, and

Glycogen synthase kinase 3 β (GSK3 β) (See Reviews by Pinto and Cleavers, 2005, Hauck et al. 2005, and Scoville et al. 2008). When β -catenin is bound to the destruction complex and phosphorylated, it is ubiquitinated and then degraded in the proteosomes. When Wnt binds to its frizzled receptor it activates “Dishevelled” which prevents the ubiquitination of β -catenin. Then β -catenin translocates to the nucleus where it binds to the T-cell factor/lymphoid enhancing-factor transcription factors (TCF/LEF) and displaces the corepressor Groucho. When β -catenin binds to (TCF/LEF) leading the transcription of Wnt target genes such as cyclin, and the C-myc oncogene, Tcf-4 null mice lack proliferating cells, have a reduction in the quality villi and are missing secretory cells. The Wnt signaling cascade plays a key role in colorectal cancers; it is currently thought that mutations in the APC gene may be the initiating event in this cancer (See Reviews by Hauck et al. 2005, and Scoville et al. 2008).

Notch Signaling Pathway

The Notch Delta lateral inhibition pathway controls large spectrums of cell fates (See Reviews by Hauck et al. 2005 and Scoville et al. 2008). The pathway involves the Notch receptor activation by the Delta or Jagged Ligand. Once activated the Ligands cause Notch receptor to be cleaved into (Notch intracellular domain) by the γ -secretase enzyme. NICD is then shuttled to nucleus where it recruits several cofactors that initiate gene transcription. This then activates the basic helix-loop-helix transcription factor hairy enhancer of split Hes1. Both Notch 1 and 2 are expressed in the crypts although Notch 2 is expressed in lesser amounts. Two Delta like proteins and Jagged 1 are expressed in the

crypts. Hes-1 knockout mice and mice treated γ -secretase inhibitors have reduced populations of enterocytes and increased populations of goblet cells and enteroendocrine cells. Both goblet cells and enteroendocrine cells express the basic helix-loop-helix transcription factor Math-1 in mice, Cath1 in chicks, and Atoh1 in humans. Math 1 is negatively regulated by Hes 1. Math 1 may act as an early secretory cell determination factor. Scoville et al. noted that in mutant NICD mice, Axin 2, a component of the β -catenin destruction complex is unaffected. This implies a permissive effect of Notch signaling on the Wnt pathway. Also of interest to note is that Math 1 can activate its own transcription and can down regulate its activity. Notch in the intestine may help to maintain stem cells as well as direct cells along the secretory lineage (See Reviews by Hauck et al. 2005 and Scoville et al. 2008).

In the avian intestine, Goblet and Enteroendocrine cells of the secretory lineage appear at approximately at 13-14 days of incubation in the basal portion of the previllous ridge (Hinni and Watterson, 1963; Black 1977). Cells of the secretory progenitor lineage express the Notch ligand Delta. In mice, the delta expression occurs in three distinct phases. At embryonic day 13.5 Delta is expressed mainly in the mesenchyme with low amounts of expression in the epithelium. At embryonic day 18.5, Delta expression is localized in the intervillous region of the epithelium. In postnatal day 25, Delta is expressed in individual cells in the intestinal crypts (Schröder, 2002). Interestingly, the classical work on differentiation from our lab seems to coincide with newer molecular data. As mentioned before, intestinal cells of the secretory lineage express the notch ligand delta (Schroder, 2002). When human cervical cancer cells that express the notch-1

receptor are cultured, in media containing varying extracellular calcium concentrations, significant changes in delta expression are observed (Raya, 2004). Raya suggests a direct mechanism where extracellular calcium concentrations are sensed by the notch signaling pathway (Raya, 2004). One could postulate where increased goblet cells in culture are due to extracellular calcium causing differential expression of the delta ligand.

Bone Morphogenic Protein (BMP) signaling

Bone morphogenic protein (BMP) binds to Type II tyrosine Kinase Receptors. This in turn, phosphorylates downstream proteins named Smads. The phosphorylation of Smad 1, 5, or 8 and then forms a heterodimeric complex with Smad, the heterodimeric complex then translocates to the nucleus and activates subsequent gene expression (See Reviews by Hauck et al. 2005 and Scoville et al. 2008). The BMP receptor 1A as well as phosphorylated Smads 1, 5, and 8 are observed throughout the villus epithelium. BMP 4 is expressed in the mesenchymal tissue surrounding the crypt in the adult and within the mesenchymal intervillus in the embryo. Furthermore, BMP 4 is localized to the +4LRC as well as near paneth cells, both of which express BMP receptor 1A. Scoville et al. suggest that BMP signals serve to antagonize crypt formation and ISC self renewal (See Review by Scoville et al. 2008). Thus BMP signaling defines crypt boundaries by controlling ISC numbers by antagonizing Wnt signals (See Reviews by Hauck et al. 2005 and Scoville et al. 2008).

Tight junctions and the Claudin Family of Proteins

Tight junctions are a defining characteristic of polarized epithelia. (See Review by Tsukita, 2000). Tight junctions behave as a primary barrier to the diffusion of solvents through the paracellular pathway in both epithelia and endothelia. The paracellular pathway is a passive system resulting from the diffusion, electrodiffusion, or osmosis down gradients that are created and maintained by the energy dependent transcellular pathway (See Review by Anderson, 2001). In ultra-thin section transmission electron microscopy tight junctions appear as cell to cell contacts involving the plasma membrane often referred to as “kissing points” (See Reviews by Anderson, 1995; Tsukita 2000). In freeze fracture microscopy tight junctions appear as intramembranous anastomosing strands or fibrils that circumscribe cells on the P-face with complementary grooves on the E-face (See Reviews by Anderson, 1995; Tsukita 2000). Tight junctions are composed of 4 main types of proteins (See Review by Anderson, 2001): scaffolding proteins like the ZO family of proteins that bind the transmembrane proteins to the cytoskeleton, signaling proteins that regulate the formation, barrier function and transcription of junctional proteins, proteins involved in regulating vesicle targeting, and finally the transmembrane proteins themselves, the latter include junction adhesion molecules (JAM), occludin, and the claudin multigene family of proteins (See Review by Anderson, 2001).

Occludin a 65 kDa protein tetraspanin protein was thought to be the primary structural component of tight junctions (See Review by Anderson, 1995). Occludin contains 2 extracellular loops that are very hydrophobic and act as tight paracellular seal.

However, it was noticed that embryonic stem cells with both alleles for occludin “knocked out” the cell were still capable of forming tight junctions (Saitou et al. 1998). Furthermore, occludin is a single protein with no extracellular charges thus, it is unable to explain the 100,000 fold variance in transepithelial resistance (TER) that can exist between different epithelia (See Review by Van Itallie, 2006). This led to further investigation of the tight junction and the subsequent discovery of a new family of proteins the claudins.

Claudin genes encode a family of proteins that are localized in the cellular tight junction, have four transmembrane domains, and a hydrophobic first extracellular loop (Furuse, 1998a). The word claudin comes from the Latin word “claudere”, which means to close. Claudins 1 and 2 were isolated from male chicken liver sucrose solutions containing tight junction proteins, in a similar manner to the occludin protein. The sucrose solution was treated with 4M guanidine to remove peripheral proteins. The solution was sonicated and subjected to a sucrose density gradient. Each sucrose fractionation was resolved, SDS page gel followed by silver staining. One band (22 kD) behaved similarly to occludin, and was found in the same sucrose interphases. The fraction containing the 22 kD band was sequenced and two full length cDNAs were produced. Claudin 1 contains 211 amino acids while claudin 2 contains 230 amino acids. Claudins 1 and 2 share 38% sequence homology to each other, and no sequence homology to occludin. Claudins one and two were colocalized with occludin by confocal microscopy. Northern blot analysis revealed that claudin 1 is expressed in the liver and

kidney, while claudin 2 is expressed in the liver, kidney and trace amounts in the brain (Furuse, 1998a).

To show that claudins are integral parts of the tight junctions, Furuse transfected L-fibroblasts with claudin cDNA molecules (Furuse, 1998b). L-fibroblasts don't form tight junction strands *in vitro*. The subcellular localization of Flag labeled claudin 1 and 2 proteins were identified using immunofluorescence microscopy with an anti-Flag monoclonal antibody. Both claudins were concentrated at cell contact sites as planes. However, the claudin localization wasn't diffusely distributed; rather it formed an elaborate network.

Next, L-Fibroblast transfectants containing claudin 1 and 2 genes were glutaraldehyde fixed and subjected to freeze-fracture microscopy. In claudin 1 transfected fibroblasts (C1FL- cells), the tight junction network was mainly associated with the P-face. The network appeared mainly continuous with some intervening spaces. The E-face contained complementary grooves with small numbers of scattered particles. Conversely, freeze fractures of L-Fibroblast transfectants containing the claudin 2 gene were discontinuous on the P-face. Claudin-2 was mainly localized on the E-face as intramembranous chains. Furuse suggested that the "tightness" of a junction can be determined by the ratio of claudin family members with claudin-1 being tighter than claudin-2 because of its association with the P-face. Furthermore, in L-Fibroblasts transfected with the occludin gene, freeze fracture microscopy revealed an absence of tight junction networks. However, when claudin-1 and occludin were cotransfected in L-fibroblasts large tight junction networks were observed by freeze fracture microscopy;

suggesting that claudin proteins are major structural components of the tight junction (Furuse 1998b).

During the same time Brizuela et al were investigating a tetraspanin transmembrane protein with two extracellular loops that was isolated from enriched *Xenopus blasutula* microsome fragments using a sucrose density gradient (Brizuela et al. 2001). They termed this protein Xcla for *Xenopus* claudin. When Xcla mRNA was transfected into L-cells (a fibroblast line that lacks endogenous tight junctions), immunohistochemistry and confocal microscopy revealed that the tight junctional protein ZO-1 was located at the cell contact points. Furthermore, when a truncated version of the Xcla which lacks the PDZ binding domain was transfected into L-cells, ZO-1 was not localized at the cell junction points. Brizuela et al. determined that the Xcla protein is important in adhesive properties of epithelial cells by injecting early *Xenopus* embryos with Xcla mRNA or the truncated Xcla mRNA. When Xcla is over-expressed, the epithelial cells adhered more tightly and cell dispersion was prevented. Furthermore, Brizuela et al. showed that Xcla proteins are required for normal embryonic development. Over-expression of Xcla mRNA or the truncated Xcla mRNA caused bilateral expression of the left-right asymmetry marker *Xenopus* Nodal-related 1 Xnr1, a left lateral plate marker. Injected embryos showed randomization in the heart, gut, and/or gall bladder (Brizuela et al. 2001).

Morita et al. described 6 new claudin proteins, three of which were previously described and designated; (RVP1 Rat Ventral Prostate 1) Claudin 3, (Clostridium Pereringens Enterotoxin-Receptor) Claudin 4, and (Transmembrane Protein Deleted in

Velo-Cardio-Facial Syndrome) Claudin 5 (Morita et al. 1999). Fifteen ESTs with similar sequence homology to claudin 1 were produced, which provided the open reading frames for claudins -3,-5,-6,-7 and -8, while mouse claudin 4 was amplified using the sequence for mouse CPE-R. Hydrophilicity plot analysis showed that claudins 3-8 were similar to claudins 1 and 2. Claudins 3-8 contain 4 transmembrane regions with NH₂ and COOH terminals in the cytoplasmic domain. The newly described proteins have two extracellular loops with the first loop being longer and more hydrophobic than the second. Northern blots of each claudin were performed in several tissues; brain, spleen, lung, liver, skeletal muscle, kidney and testes. Claudin 3 was highly expressed in the liver and lungs with only small amounts in the testes and kidney. Claudin 4 was primarily expressed in the lung and kidney while claudin 5 was expressed in all tissues with the highest levels in the lungs. Claudin 6 wasn't detected in adult tissues and its expression may be regulated in the embryo. Claudins 7 and 8 were both expressed in the lungs and kidney. Morita et al. then transfected the cDNAs of claudins 3-8 containing HA tags into MDCK cells. The HA tagged claudin antibodies were concentrated with occludin at the tight junction, in the apical part of the lateral membrane in the MDCK cells (Morita et al. 1999). To date approximately 24 claudin proteins have been described.

Claudin 16

The paracellin-1/claudin 16 gene is located on human chromosome 3q27 (Weber, 2001), and consists of 5 exons that encode a 305 amino acid protein with four transmembrane domains and intracellular NH₂ and COOH terminals (Simon, 1999).

Paracellin-1 shares 10-18 percent homology with other members of the claudin family. The highest homology is found within the first extracellular domain (Simon, 1999). Claudin 16 is localized in the thick ascending limb (TAL) of the loop of Henle, confirmed by immunohistochemistry and northern blot analysis (Simon, 1999). Using confocal microscopy, Simon confirmed that claudin 16 is colocalized with occludin, a ubiquitous tight junction protein (Simon, 1999).

The claudin 16 gene was identified by screening kindreds with a recessive form of renal hypomagnesemia, later termed Familial hypomagnesemia with hypercalciuria and nephrocalcinosis (FHHNC) (OMIM accession number 248250). Mutations in the claudin 16 gene that exacerbate magnesium wasting include premature termination, splice site, and non-conservative missense mutations (Simon, 1999). Webster et al. later screened 47 alleles finding 8 novel mutations including; five missense mutations, one frameshift mutation, and two splice site mutations (Weber, 2001). Sixty-seven percent of the mutations Weber identified affect the first extracellular domain, which is considered the bridge intercellular domain (Furse, 1998a). The first extracellular domain also shares the highest homology with other members of the claudin family (Simon, 1999). One of the novel mutations, a Leu151Phe exchange, may have a possible founder effect from Eastern Europe and Germany (Weber, 2001). The Leu151Phe mutation also affects the highly conserved first extracellular domain however; it doesn't alter the net charge (Weber, 2001).

Simon postulated that Claudin 16 is required for selective paracellular conductance. Simon et al. also proposed that claudin 16, alone or in partnership with

other proteins, forms an intracellular pore that allows magnesium and calcium to go down their electrochemical gradients and may act as a magnesium sensor. The first extracellular domain of Claudin 16 has a high density of negatively charged amino acids, with ten and a net charge of -4, and most likely acts as the pore or magnesium sensor region (Simon, 1999).

Calcium and Tight Junctions

Ma et al. determined the role of extracellular calcium in the modulation of epithelial monolayer tight junctions and delineated intracellular mechanisms involved in this process using caco-2 intestinal cells grown on permeable inserts. First, the effects of calcium free solution (0mM calcium) plus (1mM EGTA) on tight junction permeability were examined. Permeability was measured as resistance and flux. For resistance measurements a Resistance-Epithelial Voltohmmeter was used and for flux experiments mucosal to serosal flux rate of the paracellular markers mannitol and inulin was measured. Calcium free solution (CFS) produced a significant drop in transepithelial resistance (ohm-cm²) within 10 minutes, as well as increases in permeability of mannitol and inulin. Inverse relationship between flux and resistance were observed. Resistance was returned to near control levels following incubation in normal calcium levels (1.8mM) (Ma, 2000).

Thomas et al. further examined the effects of CFS on the tight junction proteins ZO-1 and occludin. The proteins were localized with anti-ZO-1 and anti-occludin antibodies, the secondary antibodies were fluorescently labeled for immunofluorescence

staining and analysis. Incubation in CFS resulted in retraction with disassembly and separation in the tight junction fence. Large gaps between the cells were observed and the protein barriers appeared “fuzzy”. The TJ fence was returned following normal calcium incubation. The effects of CFS on the cytoskeletal elements were also observed using immunofluorescence staining. Actin and myosin levels followed same trend as ZO-1 and occludin proteins (Ma, 2000).

Next, Thomas et al. examined a mechanism for the CFS modulation of the actin myosin cytoskeleton. Using precipitated Myosin Light Chain Kinase Proteins (MLCK) Thomas et al. performed *in vitro* kinase reactions to determine protein phosphorylation levels. Western blots of CFS treated Caco-2 cell show that MLCK levels weren't changed but, CFS incubation increased the phosphorylation of the myosin light chains. The inhibitor of MLCK ML-7 and several metabolic inhibitors, such as sodium azide, prevent the CFS induced retraction of the TJ. Ma et al. concluded that the CFS-induced junctional opening is mediated by the phosphorylation of MLCK, which in turn causes the contraction of the cells cytoskeleton leading to the retraction of the cell's tight junctions (Ma, 2000). However, this lab groups results may not be completely due to extracellular calcium. Black and Rogers 1992 have reported that low calcium and EDTA significantly lower intracellular calcium levels of duodenal cells. Within 30 seconds of the addition of 1.3mM calcium intracellular calcium levels increase dramatically (Black and Rogers, 1992).

In MDCK cells incubated in low calcium, the phosphorylation of occludin has been shown to be important in the reformation of the tight junctional complex (Andreeva,

2001). To determine the role of PKC in the phosphorylation of Occludin, this group used two activators of Protein Kinase C (PKC): Phorbol 12 myristate 13 acetate (PMA) and 1,2 dioctanoylglycerol (diC8). Using confocal microscopy, the localization of occludin was determined under several conditions: normal calcium, low calcium, and low calcium with PKC activators. In normal calcium (Modified Eagle's Medium, MEM with 1.8mM calcium), Occludin is localized in the junctional complexes. Under low calcium conditions (calcium free MEM), Occludin is localized primarily at the cytoplasm. When PMA or diC8 are added to low-calcium medium, occludin was partially translocated to the cell borders (Andreeva, 2001).

Next, the phosphorylation of occludin was examined by western blotting. Triton-X soluble occludin, which isn't phosphorylated appears as a single band of 60 kDa. Triton-X insoluble occludin appears as multiple bands ranging from 60-82 kDa. Under normal calcium concentrations a majority of the occludin is the higher molecular weight phosphorylated insoluble fraction. The opposite is true for the occludin of low calcium concentrations. Cells cultured under low calcium and then switched to higher calcium show an upward band shift. The same is true for cells cultured in low calcium in which PKC activators have been added (Andreeva, 2001).

The effect of the PKC inhibitor GF-109293X was then examined by Andreeva. The addition of GF-109293X to cells treated with normal calcium, PMA, and diC8 prevents the localization of occludin to the cell border. Occludin is mainly localized to the nucleus similar to cells cultured in low calcium. The addition of GF-109293X also inhibits the upward band shift of phosphorylated occludin seen in western blotting

experiments. Andreeva showed that *in vitro* recombinant occludin could be phosphorylated. Using finger printing analysis and mass spectroscopy, seronine 338 was phoshorylated. Andreeva suggested that the phosphoyrlation of seronine 338 regulates the association of occludin to the cytoskeleton. However, Andreeva was unsure if PKC directly phosphoyrlates occludin, or if other intermediate kinases phosphorylate occludin (Andreeva, 2001).

Brizuela et al. showed that claudin proteins are important for cell adhesion and are affected by calcium concentration (Brizuela et al. 2001). When Xcla mRNA is overexpressed in *Xenopus* animal caps, the cells cannot be easily dissociated by calcium/magnesium-free solution. Conversely when the truncated form of Xcla is over-expressed the cells readily dissociate (Brizuela et al. 2001).

Development of Tight Junctions in the Chick Intestine

Kimura was one of the first groups to study the development of tight junction proteins in the chick intestine (Kimura, 1996). A novel protein at the time (7H6) was isolated by collecting bile canaliculus membrane fractions from adult rats and injecting them into mice to raise antibodies. Kimura compared tight junction proteins in small intestines from E19 (19 days of incubation) and 7 days post-hatch (Kimura, 1996).

In the E19 small intestine, both occludin and ZO-1 appear as single line on the epithelial cell border resembling a “honeycomb pattern”. The same “honeycomb pattern” was observed in the in the 7-day post-hatch small intestine. The 7H6 protein had an alternate staining pattern; where at E19 it appeared as coarse dots in rows at the apical

cell border and in the 7-day post-hatch small intestine it appeared as fine dashed lines at the apical cell border, but it was discontinuous at the tricellular region, where three cells connect.

In freeze fracture electron microscopy, the tight junctions were observed at the apical portion on the intestinal cells. The tight junctions appear as belt like strands of intramembranous particles with a net like arrangement before and after hatching. The width and number of tight junctions were similar in both stages. Kimura also observed that the microvilli of the post-hatch chick were larger than those of the embryonic chick. He concluded that the 7H6 protein undergoes dramatic developmental changes after hatching whereas occludin and ZO-1 remain fairly constant. 7H6 may play a role in colocalizing with other tight junction proteins during the ontogeny of the intestine (Kimura, 1996).

A descriptive study of the localization of several claudin proteins was performed by Ozden while working in the laboratories of Black and Grubb (Ozden et al. 2004). Using polyclonal antibodies against claudins 3, 5, and 16, the expression pattern of each protein was examined in the three regions of small intestine. The study examined the localization of claudin proteins in 1-day old hatched chicks as during the week prior to hatching (Ozden et al. 2004).

The Expression Pattern of Claudins 3, 5, and 16 in the One Day Old Chick Intestine

In the 1-day old chick, all three claudins examined were present in duodena, jejunal, and ileal regions of the small intestine (Ozden et al. 2004). Claudin 5 staining

was present in the apical cell-to-cell contact regions, the terminal web of the crypt region, and on the lower portion of the villus, after which it becomes restricted to the terminal web of the villus tip. In longer more mature villi, a gradient of claudin 5 staining was observed along the crypt to tip axis, with more intense staining at the villus base. In shorter less mature villi, no staining gradient was observed. Ozden speculated that in mature intestine claudin 5 may play a role in cellular proliferation and may contribute to the migration of cells up to the villus. Furthermore, the lack of claudin 5 staining at the villus tip correlates to the region of the villus in which cells slough off. Ozden hypothesized that claudin 5 may play a role in the secretion of water and ions by forming paracellular pathways in the lower region of the villus.

Claudin 3 staining was noted in the epithelium that is in the closest contact to the basement membrane. Claudin 3 staining was also noted in mainly in the lateral membrane and apical cell to cell contact regions of the epithelium. Some staining was present in the cytoplasm of cells on lower portion of the villus, but not in the crypt regions. Ozden concluded that claudin 3 may be located in the lateral junctional complex, perhaps with desmosomes and E-cadherins, and via interactions with other claudins might contribute to increasing the “tightness” of the junctions. The staining observed near the basement membrane might aid in the attachment of the epithelium to the basement membrane. Ozden also noted that less claudin 3 was present near the cell extrusion zone of the villus tips and that no claudin 3 was present in the crypt region where cell to cell contacts are loose. Interestingly, claudin 3 staining was noted in the cytoplasm of some

cells. When occludin is unphosphorylated and localized in the cytoplasm (Andreeva, 2001), this may allow for greater cell movement.

Claudin 16 staining was present in goblet cells in a gradient increasing along the crypt to tip axis (Ozden et al. 2004). Little staining was observed in the bottom portion of the villus, while the staining was strongest at the tip region of the villus. In some cells the mucin granules were outlined by staining that suggests that claudin 16 was localized within the granule membranes. The authors suggested that claudin 16 within the mucin granule might play a role in calcium related mucus secretion. Lastly, some apical and junctional staining was observed within the epithelium. Thus it was concluded that claudin 16 might have a role in the absorption of calcium and magnesium by paracellular pathways, in a similar manner to the kidney tubule epithelium (Ozden et al. 2004).

The Development of Claudins 3, 5, and 16 in the Embryonic Chick Intestine

The development of claudins 3, 5, and 16 was examined in the week prior to hatching in the embryonic small intestine (Ozden et al. 2004). The proteins were examined every two days from days 12-20, in most cases.

The 12-day old embryonic duodenum, jejunum and ileum stained with claudin 3 the upper portion of the villus stained more intensely than the villus bases, and cytoplasmic staining was also observed. In 14 day old intestine, claudin 3 staining was more intense in the villus tips when compared to 12 days, suggesting that it contributes to strong cell adhesion and the formation of the developing ridges at this time. At 18-days, some staining of cytoplasmic granules was observed. At 20-days the staining appeared

more concentrated near the cellular membranes, suggesting that the maturation of tight junctions had occurred.

Claudin 5 was present in the intestinal epithelial layer at 12-days of embryonic development, staining increased in intensity through 20-days and became localized in the apical cell contact regions. In contrast, Claudin 16 could not be observed by immunostaining until 20 days of development. The authors suggested that goblet cells from 14-18 day old intestine lack stimulated exocytosis, and that claudin 16 appears when the goblet cells are functionally mature. Additionally, claudin 16 may play a role in calcium-regulated goblet cell differentiation by acting as a calcium channel subunit (Ozden et al. 2004).

Claudin Localization and Development in the Mammalian Gastrointestinal Tract

Rahner and co-workers developed synthetic peptides against claudins 1-6; rabbit polyclonal antibodies were raised against each peptide and affinity purified by Zymed laboratories (Rahner, 2001). Immunohistochemistry was performed on the following organs in rats: liver, pancreas, small intestine and large intestine. Claudin 2 was restricted to the intestinal crypts in both the small and large intestine. Claudin 3, on the other hand, had no obvious crypt-villus gradient in total staining. In the small intestine, claudin 3 localized in the junction of the intestinal crypts, however at the villus tip basolateral staining was observed in the epithelium. Claudin 4 staining was highest in the surface epithelial cells of both the small intestine and large intestine. Claudin 4 staining was

laterally, but not specifically in junctional regions. Claudin 5 was observed in the tight junctions of enterocyte epithelium and did not show a crypt villus tip gradient.

In immunoblots of claudins 2-5 all four antibodies appeared in the duodenum, ileum, and colon at differing levels (Rahner, 2001). Claudin 3 and 4 were observed in the jejunum and 2 and 3 in the liver, while none of the claudins appeared in the stomach. This group made three conclusions about claudins and their function in the gastrointestinal tract; 1) claudins and tight junctions in the gastrointestinal tract are varied and complex, 2) gradients in paracellular transport are graded and increase in complexity along the crypt-villus tip axis, 3) claudins are located along the epithelial lateral membranes. Rahner and colleagues speculated that claudins can influence ion or solute movement along the lateral intracellular space and that lateral staining may also represent a storage pool for additional claudins, furthermore, thus indicating an additional non-barrier function (Rahner et al. 2001).

In 2006 Holmes and co-workers examined claudin profiles along the mouse gastrointestinal tract (Holmes et al. 2006). In adult mouse intestine, quantitative PCR revealed that claudin 1-5, 7-15, 17 and 18 are expressed in the intestine, while claudins 2, 3, 7 and 15 were more highly expressed. In immunohistochemistry claudin 2 was expressed in the deep crypt while claudin 10 was expressed along the entire crypt. Claudins 7 and 8 were expressed uniformly along the crypt-villus axis, and claudin 4 in the upper villus and sporadically in the deep crypt.

During development of the mouse gastrointestinal tract, mRNA levels of claudin 2 decrease from birth to 90 days by 10 fold. Claudins 3, 4, 7 and 15 increases after birth

to 90 days by 2 to 20 fold, with the greatest changes in expression occurring during weaning 14-28 days. At postnatal day 1, claudin 15 is predominantly in the crypts but progresses up the villus length by day 28. At postnatal day 1, claudin 2 is ubiquitously expressed along the crypt-villus axis; then at 28 days it becomes restricted to the crypts. This group suggested that this study is a base for those interested in claudins and their role in differentiation, transport and disease (Holmes, 2006).

Section II. Materials and Methods

Isolation of Epithelial Cells from Intestinal Villi:

Fertile eggs of the broiler strain were obtained from the Poultry Science department at NC State and incubated at 37°C in a force draft incubator with automatic egg turner for 18, 20 embryonic or one and two days post-hatch. All duodenal loops were removed and immediately placed in ice-cold phosphate buffered saline (PBS) at pH 7.4. All pancreas and mesenteries were removed and discarded. The duodena were then cut in half split to expose the epithelia to the buffered solutions. The following numbers of duodena were collected for the epithelial cell isolation for each age: 18 days, 16 duodena; 20 days 8-10 duodena; 2 days post-hatch, 2-3 duodena. Adult chicken intestine was obtained from the Poultry Science department at NC State and were used to obtain duodenal or ileal epithelial cells. All duodena were kept in PBS over ice until all dissections were complete. Following dissection, the split duodena were placed in room temperature citrate buffer containing 1.5mM KCl, 96mM NaCl, 27mM Sodium Citrate,

8mM KH_2PO_4 , and 5.6mM Na_2HPO_4 for 15 minutes. Tissues were then transferred into 25ml erlenmeyer flasks containing 2.2ml of Buffer B consisting of 128mM NaCl, 10mM Na_2HPO_4 , 1.4mM EDTA, and 0.5mM Dithiothreitol. Tissues were then incubated in a Dubnoff metabolic shaking incubator at 37°C at 120 cycles/minute. Duodena from 18 day and 20-day old embryos and from hatched chicks were shaken for 30 minutes to collect the entire villus. The contents of each age group were then pooled before sonication. When the crypt/villus fractions were isolated from 20-day old post-hatch chicks, the duodena were moved to new Buffer B after 0.5, 10, 20 and 40 minutes of shaking. The 0.5 minute fraction was usually discarded as it contained the dying tip cells. The remaining fragments contained the upper villus, lower villus and crypt epithelium, respectively (Grimes and Black, 1987). The cell suspensions were then filtered through a silk screen to remove any debris and centrifuged for 5 minutes in a table top centrifuge. The supernatant was discarded and the cells were then washed in ice-cold PBS and frozen for storage at -20°C. Rat kidneys used for a positive control for claudin 2 and claudin 4 were graciously provided by Dr. Robert Grossfeld. Bird kidneys were obtained when the NCSU poultry science department sacrificed adult birds. The kidneys were homogenized in ice-cold PBS and stored at -20° for later use.

Western Blotting

Thawed cells were then washed again and sonicated for a total of 30 seconds. The protein concentration was measured at A 280 on a Nanodrop 1000TM. Each sample was assayed in triplicate and averaged. 33µl of 4xSDS was added to 100µl of lysate and

sonicated again, then diluted to final concentrations with 1xSDS. The remainder of the protocol was modified from (Tipsmark et al. 2007). Final protein concentrations of were 10ug were loaded for ERK gels, 30ug for Claudin 2 and 60ug to 75ug for Claudin 4. ERK and claudin 2 were run side by side, in blots of with ERK as a control for equal loading as it is approximately equivalent in crypt and villus fractions in adult chickens (Mamajiwalla and Burgess, 1995) and remains constant throughout small intestinal development in rats (Marandi et al. 2002). Sample buffer and sample reducing agent (NuPAGE, Invitrogen, San Diego, CA) contained 141mM Tris Base, 106mM Tris HCl, 73mM LDS, 0.5mM EDTA, 50mM dithiothreitol and: 8% glycerol (v/v), 0.019% serva blue G250 (w/v), 0.006 phenol red (w/v). Samples were then heated at 80°C for 10 minutes prior to loading. Samples were separated by gel electrophoresis using 12% Bis-Tris, 1.0mm X 17well gels (NuPage system) and MES/SDS running buffer containing 50mM 2-(N-Morholino) ethanesulfonic acid, 50mM Tris, 3.5mM SDS, and 1mM Na₂-EDTA with the addition of 500ul of NuPage antioxidant to the inner chamber at 200 Volts (Xcell II; Invitrogen) for 35 minutes. Molecular weight was estimated using a prestained marker (BioRad, Hercules, CA). Protein gels were then uncast and washed in transfer buffer containing 25mM Tris, 192mM glycine, 10% methanol (v/v) on a shaking platform for 15 minutes to remove running buffer. Following the washing step, the gel was blotted on a 0.45µM nitro-cellulose membrane (Invitrogen) by submerged blotting for 1 hour at 30 volts (Xcell II; Invitrogen) in transfer buffer. Membranes were then blocked in Odyssey Blocking Buffer (Li-Cor, Lincoln, NE) for 1 hour on a shaking platform. Membranes were then incubated in either 1:2000 ERK 1 (K-23) (Santa-Cruz

Biological, Santa Cruz, CA), 1:250 claudin 2 (Invitrogen) or 1:250 Claudin 4 (Invitrogen) primary antibodies in Odyssey Blocking Buffer (Li-Cor, Lincoln, NE) at 4°C on a shaking platform overnight. Membranes were then washed 4 times in PBS with 0.1% Tween 20 for 5 minutes each and incubated for 1 hour with secondary antibodies conjugated to Alexa IR Dye 680 or Alexa IR Dye 800 (Li-Cor, Lincoln, NE) at a final concentration of antibody 1:10,000 in Odyssey Blocking Buffer (Li-Cor, Lincoln, NE) in a dark room. Membranes were briefly washed in PBS to remove excess Tween-20 before being scanned and analyzed on the Odyssey Infrared Imaging System (Li-Cor, Lincoln, NE). Integrated intensity values were determined by the Odyssey 2.1 scanning software, data was then exported into Microsoft Excel files for graphing and data analysis.

Section III. Results

A Western blot with several protein concentrations was run with the Zymed Claudin 2 antibody to determine its specificity and to determine proper protein concentrations to load on subsequent gels. The blot contained 20ug, 50ug, and 100ug of rat kidney homogenate (as a positive control), adult chicken duodenal epithelium and ileal epithelium. The claudin 2 band was located correctly at the 20Kd molecular weight, the third band from the bottom refer on the BioRad precision molecular weight marker gel (Figure 2 A,B,C). Integrated intensity values for claudin 2 in the kidney control for 10ug, 50ug, and 100ug of homogenate were 39, 139, and 181 pixels mm², respectively (Figure 2D). Increases in integrated intensity with increasing protein concentration were also seen in the duodenal and ileal epithelium. The duodenal epithelium appeared to contained more claudin 2 per ug of protein than the ileal epithelium. All further studies utilized epithelium from the duodena.

Western blots with claudin 4 homogenates containing multiple protein concentration were also run using cells from the crypt-villus axis of hatched chicks. Amounts of protein from 10 - 100ug micrograms were tested (data not shown) and it was determined that 60 - 75 ug of protein was optimal considering the low levels of claudin 4 expression in the small intestine.

Next, the ontogeny of both ERK 1 and claudin 2 during the 3 days preceding and two days following hatching was investigated. ERK 1 was chosen as a sample loading control as it changes little during development in rat small intestine (Marcial, 2005) as

well as being approximately equivalent at different levels of the crypt-villus axis in adult birds (Mamajiwalla and Burgess, 1995). The ERK 1 (K23) antibody (Santa Cruz biotechnology, Santa Cruz, CA) recognizes both ERK 1 and 2, the latter to a lesser extent. Both ERK 1 and 2 were located at the correct molecular weight markers 44 and 42Kd, although ERK 2 was often undetectable. ERK 1 and claudin 2 were both detected in 18-day embryos, although the claudin 2 band was faint (Figures 3 and 4). Claudin 2 expression was stronger at 20 days of incubation in the duodenum than at 18 days and had the greatest expression in epithelium from 2-day old chicks (Figures 6 and 8). In contrast, ERK 1 expression was fairly constant over the same developmental period, but appeared to have a slightly higher expression at 2-days post-hatch (Figure 7).

Next, the expression of ERK 1 and claudin 2 were examined along the crypt-villus axis of 2-day post-hatch chick duodenal epithelial cells. ERK 1 showed no difference in expression along the crypt to tip axis in 2-day post-hatch chicks (Figure 9). In contrast, claudin 2 showed a pronounced gradient at different levels of the villus, with the greatest expression in crypt cells (Figure 10). The integrated intensity values for claudin 2 ranged from 0.56 units in the upper villus cells to 2.23 units in the crypt. It was of interest to determine how early in development the claudin 2 crypt-villus gradient appears. Figure 12 shows that the gradient is present at 20 days of embryonic development when crypts are beginning to form. ERK 1 showed no obvious gradient, but cells from the upper villus had somewhat lower levels of ERK 1 than cells from the lower villus and crypts (Figure 11).

Detection of claudin 4 in duodenal epithelial proved difficult, even when large amounts of protein (60-100 ug) were used in Western blotting. Claudin 4 at the correct molecular weight of ~20Kda was not detected in epithelium from duodena of 18-day embryos, 20-day embryos, or 2-day old hatched chicks, although a band was seen in 18-day embryos at ~14Kda (Figure 13). Likewise, no clear claudin 4 band was seen in epithelium along the crypt-villus gradient of 2-day old chicks (Figure 14). In order to determine whether claudin 4 was expressed later in post-hatch development, Western blotting was performed on duodenal epithelium from 3-week old chickens. To see if this immunoblotting technique could detect claudin 4 in chickens, *per se*, a homogenate of chicken kidney was run in addition to that of rat kidney. A band corresponding to the correct molecular weight of claudin 4 was observed in epithelial cells isolated from the entire villus as well as in fractions obtained after different time periods of shaking the intestine in EDTA-buffer (Figure 15). The origin of cells along the crypt-villus tip axis has not been established for birds older than 2 days in the protocol used, so there is no way to verify the level of crypt/villus for these cells. However, it is almost certain that the cells in fraction 1 (30 sec shaking) originated from the villus tip. Interestingly, chicken kidney showed a claudin 4 band at the same molecular weight as rat kidney, but also had 2 additional bands of lower molecular weight. One of these (~14Kda) appeared to be the same band as seen in the duodenal epithelium of 18-day embryos. The same band was present in the 3-week chicken duodenum. Further Western blots using 3-week chickens revealed that of claudin 2 and ERK 1 are also expressed in duodenal epithelium (Figures

16 and 17). Additionally, ERK 2 was visible as a very light band, similar to 2 days post-hatch. ERK 1 and 2 were present in chicken kidney, but claudin 2 was not detected.

Section IV. Discussion

This research has investigated the ontogeny and expression along the crypt-villus axis of claudin 2, claudin 4, and ERK 1 in the embryonic and early post-hatch epithelial cells of the chick intestine. The ERK 1 protein was utilized as an internal control because its expression was not expected to change much during late developmental stages. It has been demonstrated that total immuno-precipitated ERK 1 and 2 do not increase during 10 to 40 days postpartum in neonatal rat intestine (Marandi et al. 2002). In adult chicken intestine, ERK is located within villus and crypt fractions of adult bird intestine in approximately equivalent amounts (Mamajiwalla and Burgess, 1995). This made ERK 1 seem a good candidate for sample preparation control, even though ERK 1 expression had not previously been examined in embryonic and young chick intestine. In the current work, ERK 1 levels increased only slightly during the 5-day period between 18 days of embryonic development and 2 days post-hatch, and there was no discernible gradient in ERK expression from crypt to villus tip in the intestinal epithelium of hatched chicks.

In the same epithelial preparations, claudin 2 was barely detectable in duodena from 18-day embryos, became more obvious at 20 days, and increased dramatically by 2 days post-hatch. Increased expression of claudin 2 between 18 and 20 days of embryonic development probably reflects the formation of crypts (which is just beginning at 20 days), whereas the subsequent increase in expression may be a function of increase in crypt surface area and density. Examination of claudin 2 levels along the crypt-villus axis in 20-day embryos confirmed that most of this protein was in fact located in the crypt

cells, and in 2-day old chicks there was a pronounced villus-tip gradient with highest claudin 2 levels in crypt epithelium.

Consistent with this interpretation, Uni et al. (2000) reported that each villus had approximately one small crypt containing few cells in newly hatched chicks. Histological studies revealed that crypts then grew rapidly; crypt perimeter and number of cells per crypt increased until 120 hours post-hatch. Uni and colleagues demonstrated that cell hypertrophy increases by approximately 20% in the intestinal crypt. Just before hatch, all cells along the intestinal villus were PCNA positive, but after hatch PCNA cells were increasingly located within the crypts. Furthermore, almost all cells on the villus were Brdu positive (in the process of mitosis) at 24 hours post-hatch, but by 44 hours a majority of the Brdu cells were observed in the crypts. Uni et al. suggested that the first post-hatch day marks a transition from crypt growth to the commitment to produce mainly enterocytes (Uni et al. 2000). The increase of the claudin 2 in the crypts during the same time frame might reflect this commitment towards adult function.

Figure 10 reveals a pronounced crypt-villus gradient of claudin 2 in duodenal epithelium from 2-day old chicks. Many proteins show gradients along the crypt-villus axis. For example, Mariadason et al. (2005) analyzed gene expression in epithelial cells along the crypt-villus axis of adult mice and reported that 1113 genes were differentially expressed along the crypt villus axis. In their study, the claudin 2 gene was down regulated at the villus tip (Mariadason, 2005). The Western blots of Figure 10 are in general agreement with Mariadason's findings. Other studies have also indicated that claudin 2 becomes preferentially localized to the crypts during development. Rahner et al.

(2001) used immunohistochemistry to demonstrate claudin 2 localization in the crypts of adult mice. Immunofluorescent antibodies have been used to demonstrate that in new born mouse intestine, claudin 2 is uniformly expressed along the villi and crypt, but becomes localized within the crypts by day 28 postpartum (Holmes et al. 2006).

The promoter activity and regulation of the claudin 2 gene has been well studied. Claudin 2 is located on chromosome X q223.23. Its promoter contains no TATA box, but it does contain a CAAT box and two E-boxes (Sakaguchi et al. 2002). The promoter of claudin 2 contains two sites for Cdx homeodomain binding and a site for hepatocyte nuclear factor 1 alpha (HNF-1 α) binding. Cdx 2 expression induces strong promoter activity while HNF-1 α in combination with Cdx 2 increases promoter activity in Caco-2 cells. In HNF-1 α deficient mice, Cdx 2 expression was required for the expression of claudin 2 in the liver; however it was not required expression in the kidneys. In HNF-1 α mice, claudin 2 is absent from the villus, but it is still expressed in the crypts. The authors suggest that HNF-1 α may coordinate with additional factors in the intestine to regulate claudin 2 (Sakaguchi et al. 2002). Further examination of the claudin 2 promoter revealed it contains binding sites for two effectors of the Wnt signaling pathway LEF/TCF (Mankertz et al. 2004). This group transfected claudin 2 reporter gene constructs into C57 cells that stably express Wnt-1 and cells that don't express Wnt-1. Claudin 2 promoter activity increased in the cells that stably express Wnt-1. Claudin 2 promoter activity was increased when TCF 4 or β -catenin were co-transfected with the claudin 2 promoter in HEK 293 cells. When the LEF/TCF site was mutated by site directed mutagenesis, claudin 2 promoter activity was reduced. Furthermore, when Cdx binding sites are

mutated a decreased response is observed in β -catenin and LEF-1 mediated claudin 2 promoter activation. The authors suggest a model in which LEF-1/ β -catenin activate the claudin 2 promoter both directly and indirectly to regulate claudin 2 and possibly other claudins (Mankertz et al. 2004).

The development of Cdx genes have been examined in pre- and post-hatched birds (Sklan et al. 2003). Chicks express CdxA which shares 95% homology with the mammalian Cdx2. CdxA mRNA is low at 15 days of incubation, and increases are observed from 17 days incubation until hatching. In the post-hatch chick, small increases are observed in CdxA expression (Sklan, 2003). This coincides nicely with our observations of claudin 2 expression. The claudin 2 protein was detected in the duodenal epithelium at 18 days, although at low levels. At 20 days and 2 days post-hatch, claudin 2 expression was markedly increased. One could propose a mechanism in which the avian homolog to Cdx2 (CdxA) binds to the claudin 2 promoter around 17 days incubation, then induces claudin 2 expression around 18 days which continues to increase until hatching. It would be interesting to examine even younger embryos. However, this would require large amounts of embryonic intestine tissue to yield enough epithelium for analysis.

As discussed in the introduction, components of the Wnt signaling pathway are expressed in the mature crypts of mammalian intestine (See Reviews by Pinto and Cleavers, 2005, Hauck et al. 2005, and Scoville et al. 2008). A gradient of Wnts exists which decreases in intensity from crypt to villus tip. This may further explain the decreasing claudin 2 gradient up the crypt-villus axis. Furthermore, Wnt activity has been

examined in TOP-GAL and Axin2^{LacZ} transgenic mice. Wnt activity is found exclusively within the villus epithelium of 16-day embryos and is not seen within the intervillus region until postnatal day 2 (See Review by Scoville et al. 2008). This may explain the previous observation that claudin 2 is localized along the entire villus in 1-day old postnatal mice (Holmes et al. 2006). Taken together, the embryonic expression patterns of the Wnt pathway and CdxA homeobox genes may explain the expression pattern of claudin 2 that was observed in chick intestine in the present study.

As described in the introduction, claudin 2 has been associated with "leaky" tight junctions and with paracellular movement across the intestinal epithelial barrier. Rahner et al. (2001) inferred that paracellular transport is graded and has an increasing complexity along the crypt-villus axis. Gradients of different claudins could explain these differences in transport function. Marcial et al. (1984) used combinations of light microscopy, TEM, SEM and mathematical theorem to relate tight junctional structure to paracellular resistance. This group concluded that the villi account for almost 90% of epithelial surface area. However, when junctional length and densities are taken into account, the crypts contribute 73% of paracellular conductance. Transmission electron microscopy revealed that there are approximately three times more junctions per mm of surface in the crypt; 384 in the crypt epithelium compared to 109 in villus epithelium. Marcial et al. speculate that the geometry of tight junctions in the crypt is the structural basis for paracellular movement of Na⁺. Claudin 2 can act as a cation pore as it contains 3 negatively charged amino acids in its first extracellular loop (VanItallie et al. 2003). At physiological pH, most claudins are cation selective (See Review by Anderson, 2001). In

leaky epithelium like the intestine, the paracellular pathway is a major component of overall transport and changes in charge have great impacts on overall compositions of fluids. Claudin 2 is considered a “leaky” tight junction and its localization in the crypts at 20 days in embryonic chick duodena may establish the adult pattern of tight junctions and prepare the intestine for the absorptive functions required soon after hatching.

Claudin 4 is considered a “sealing” claudin which decreases the paracellular permeability through tight junctions, it was chosen in the present study because it has properties opposite of claudin 2 (See Review by Krause, 2007). Regarding the mammalian intestine, claudin 4 is highest in the surface epithelium cells of the small and large intestine (Rahner et al. 2001). Holmes et al. (2006) noted that claudin 4 was located in the upper villus region, but sporadically found within the deep crypts. This group used quantitative PCR to show that claudin 4 is expressed, although low levels of transcripts were detected. In developing mouse intestine, claudin 4 had the highest levels of expression at 90 days postpartum. Claudin 4 wasn't detected until the duodenal epithelium of older birds was examined (Figure 15). Thus it is likely that this claudin is not expressed at significant levels until some time between 3 and 21 days post-hatch, perhaps after the chicks begin to feed. Based on the distribution of claudin 4 in mammalian intestine, it was expected that claudin 4 would be higher in villus epithelium than in the crypts of hatched chicks. Unfortunately, our protocol for sequential cell isolation has only been validated for intestine from 20-days of embryonic development through 2-days post-hatch. While "fractions" of epithelial cells from the 3-week old birds were collected, the cell populations have not been characterized, and it is possible that

villus and crypt cells are present in all fractions except those from the villus tip (obtained after only 0.5 min of shaking). As expected, the villus tip cells gave strong bands for claudin 4 protein.

Although a mouse monoclonal antibody for the Western blots of claudin 4 was utilized in the present study, the antibody data sheet noted reactivity in chick. The monoclonal claudin 4 antibody detected additional bands with a lower molecular weight than claudin 4, which were most prominent in epithelium from 18-day embryos and from the crypts of 2-day old chicks (Figures 13 and 14). The lower molecular weight bands were also present (in addition to claudin 4 bands) in epithelium from 3-week old chickens and in homogenates of chicken kidney, although only a single band with correct molecular weight for claudin 4 was found in rat kidney (Figure 15). It is possible that these lower molecular weight bands are degradation products of claudin 4, but the low molecular weight bands may also represent a claudin-like protein expressed in both bird kidney and intestine that this particular antibody recognizes. In the latter case, the protein may be associated with immature enterocytes as found in embryonic intestine and in the crypts of post-hatch chicks. Further studies are required to form a definitive conclusion about the expression of claudin 4 during ontogeny and along the crypt-villus axis.

Claudin proteins play an important role in the tight junctions of intestinal epithelium, but the function of a specific claudin can depend on the cellular background of other claudins present (Hou et al. 2006). For example, claudins 4 and 7 can have a different properties depending on the cell line in which they are expressed. Claudin 4 and claudin 7 can act either as a barrier to sodium or as channel to calcium ions. When

MDCK cells are transfected with either claudin, these cells become barriers to cations even though this cell line is normally cation selective due to the expression claudin 2. In LLC-PK1 cells, which are anion selective, claudins 4 and 7 act as paracellular chloride channels. LLC-PK1 cells endogenously express claudins 1, 3, 4, and 7 with little claudin 2 expression. Thus it is likely that the functions of claudins 2 and 4 in developing chicken intestine are influenced by the expression pattern of other claudins and claudin-like proteins.

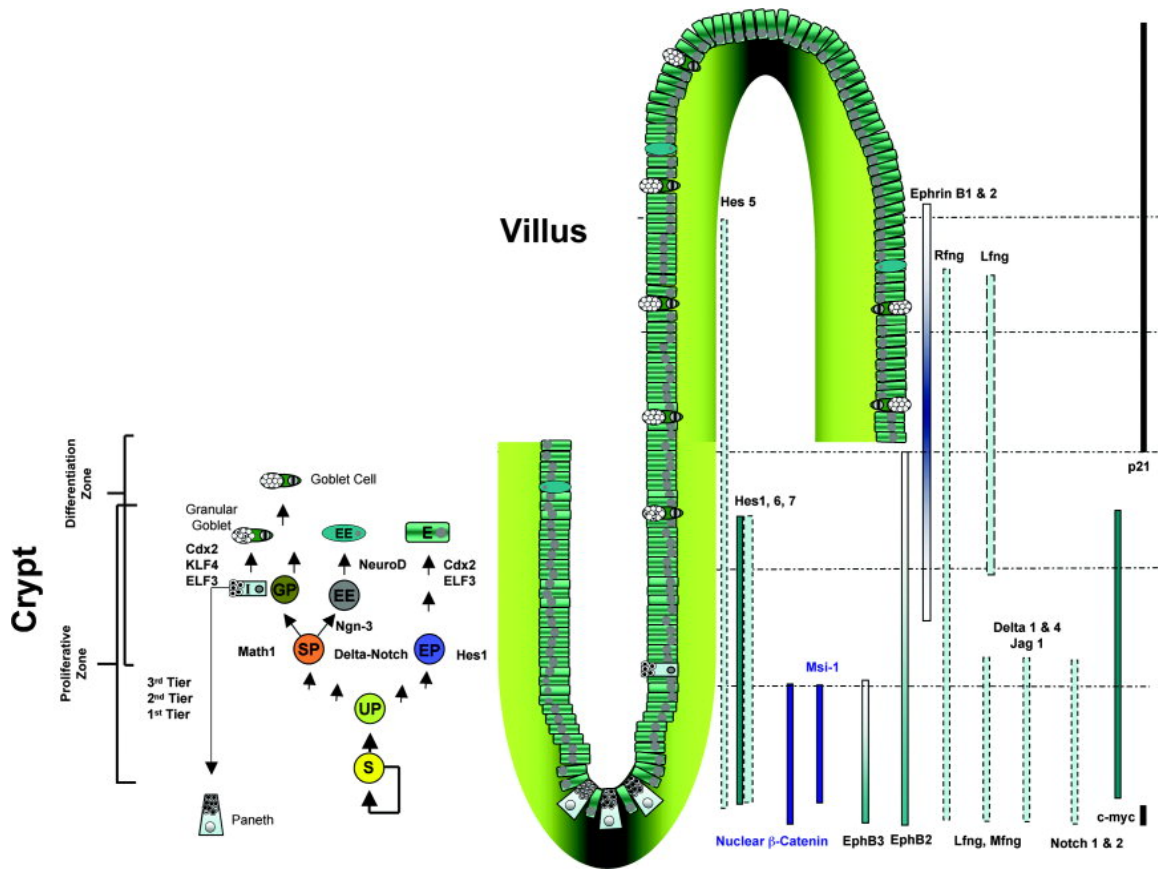


Figure 1. Proposed mechanism for the maintenance and renewal of the crypt-villus axis.

(Figure is from review by Hauck et al. 2005)

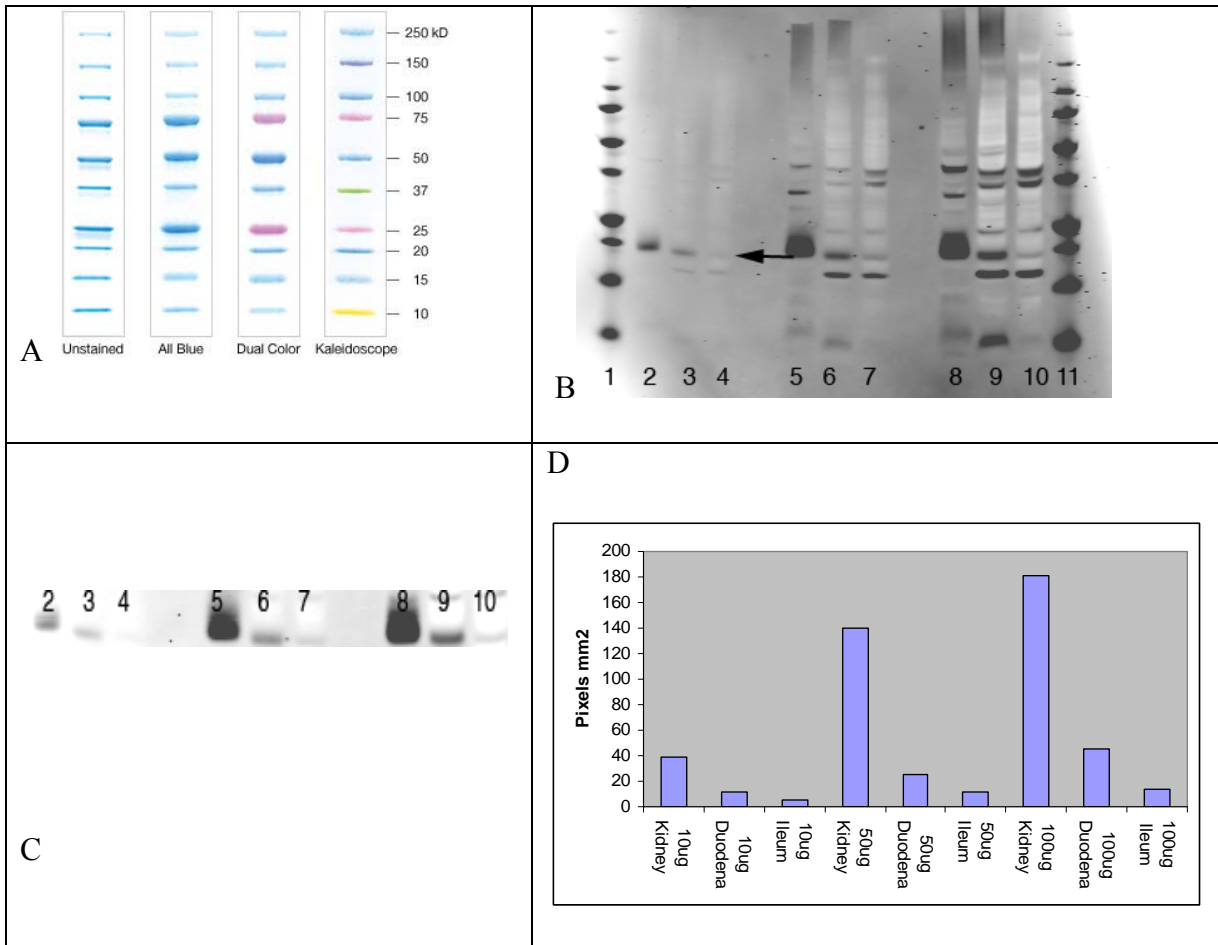


Figure 2. Claudin 2 in rat kidney and intestinal epithelium of adult chicken

Figure A. BioRad Precision Molecular weight marker (Hercules, Ca). Figure B. Odyssey Scan of claudin 2 immunoblot. Claudin 2 Immunoblot Lanes are as follows: Lane 1) Molecular weight marker, Lane 2) 10ug of rat kidney, Lane 3) 10ug duodenum, Lane 4) 10ug ileum; Lane 5) 50ug of rat kidney, Lane 6) 50ug duodenum, Lane 7) 50ug Ileum; Lane 8) 100ug of rat kidney, Lane 9) 100ug duodenum, Lane 10) 100ug ileum; Lane 11) Molecular weight marker. Claudin 2 bands appear below the 20Kda molecular

weight marker the third band 3rd up from the bottom as indicated by the arrow. Figure C.
Cropped image of Claudin 2 bands from figure B, lanes 2-10. Figure D. Integrated
Intensity units in pixels per mm² (N=1).

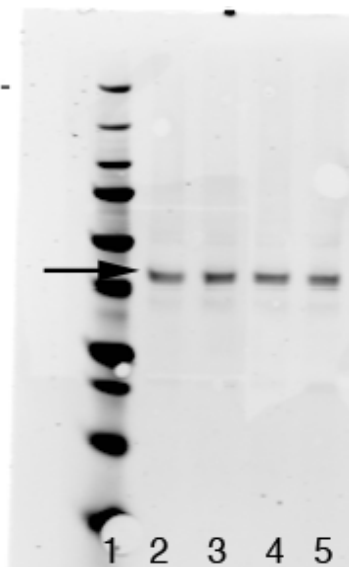


Figure 3. ERK 1 expression in embryonic duodenal epithelium at days 18 of development.

Odyssey scan of ERK 1 immunoblot. Lanes are loaded as follows: Lane 1) Molecular weight marker, Lanes 2-5) 10ug duodenal epithelium (N=4).

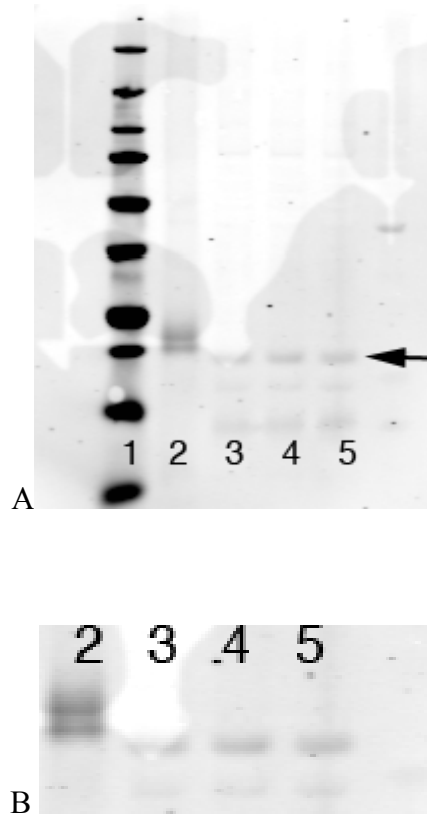


Figure 4. Claudin 2 Expression in embryonic duodenal epithelium at 18 days of development

A. Odyssey scan of claudin 2 immunoblot. Lanes are loaded as follows: Lane 1) Molecular weight marker, Lane 2) 30ug of rat kidney positive control, Lanes 3-5) 30ug duodenal epithelium. B. Crop of claudin 2 bands, lanes 2-5 (N=3).

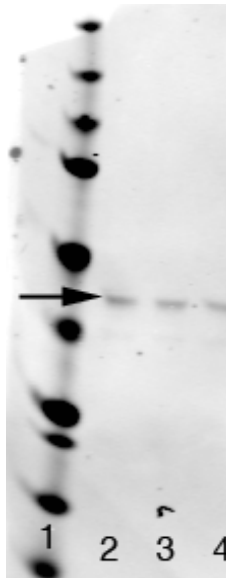


Figure 5. ERK 1 expression in embryonic duodenal epithelium at 20 days of development
Odyssey scan of ERK 1 immunoblot. Lanes are loaded as follows: Lane 1) Molecular
weight marker, Lanes 2-4) 10ug 20 day duodenal epithelium (N=3).

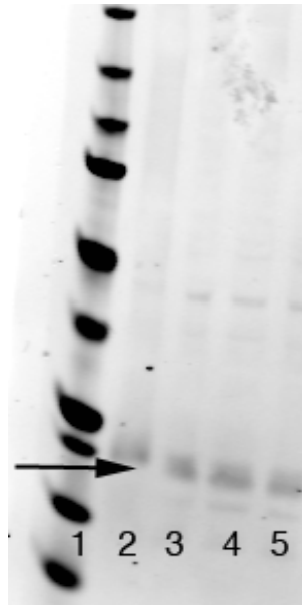


Figure 6. Claudin 2 expression in embryonic duodenal epithelium at 20 days of development

Odyssey scan of claudin 2 immunoblot. Lanes are loaded as follows: Lane 1) Molecular weight marker, Lane 2) 30ug rat kidney positive control, Lanes 3-5) 30ug duodenal epithelium (N=3).

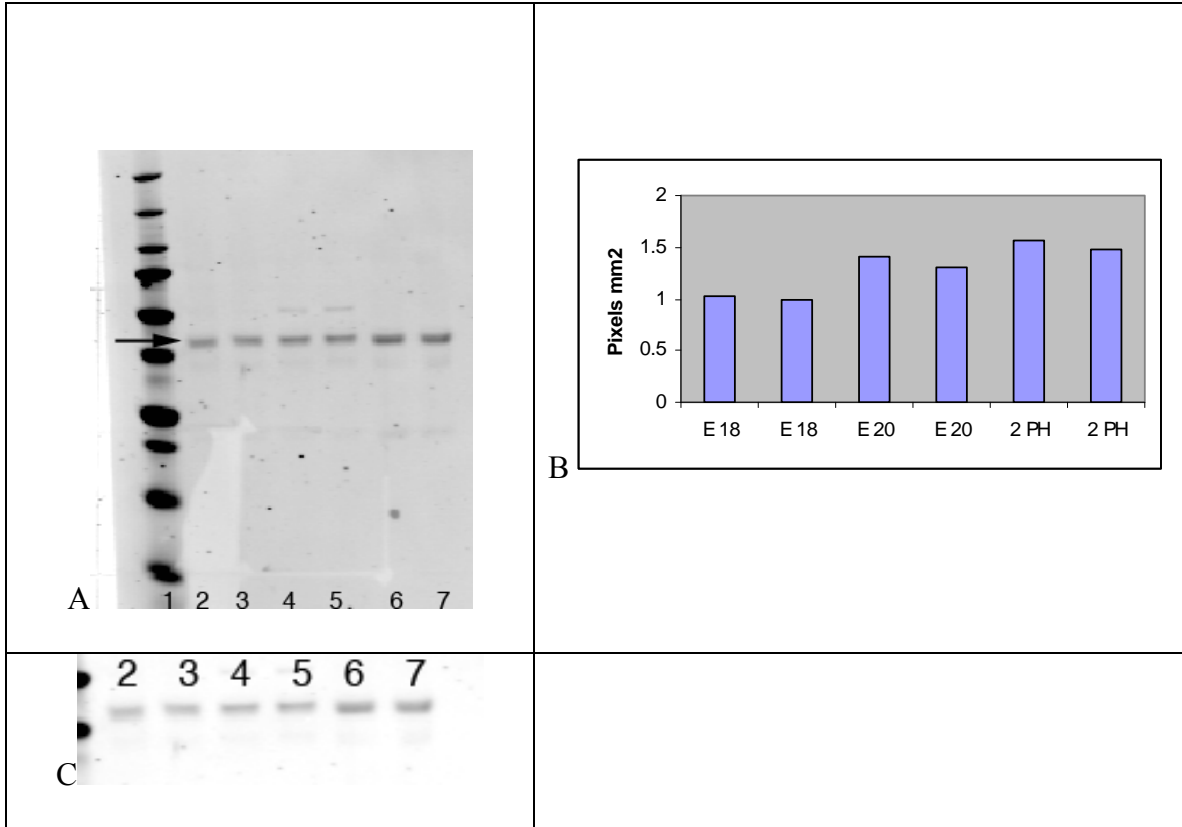


Figure 7. ERK 1 expression in duodenal epithelium from pre- and post-hatch chicks

Figure A. Immunoblot of ERK1. Lanes are loaded as follows: Lane 1) Molecular weight marker, Lanes 2-3) 10ug 18-day duodenal epithelium, Lanes 4-5) 10ug 20-day duodenal epithelium, Lanes 6-7) 10ug 2-day post-hatch duodenal epithelium. Figure B. Integrated intensity values from ERK1 immunoblot values expressed as pixels mm². Figure C. Crop of ERK 1 bands Lanes 2-7.

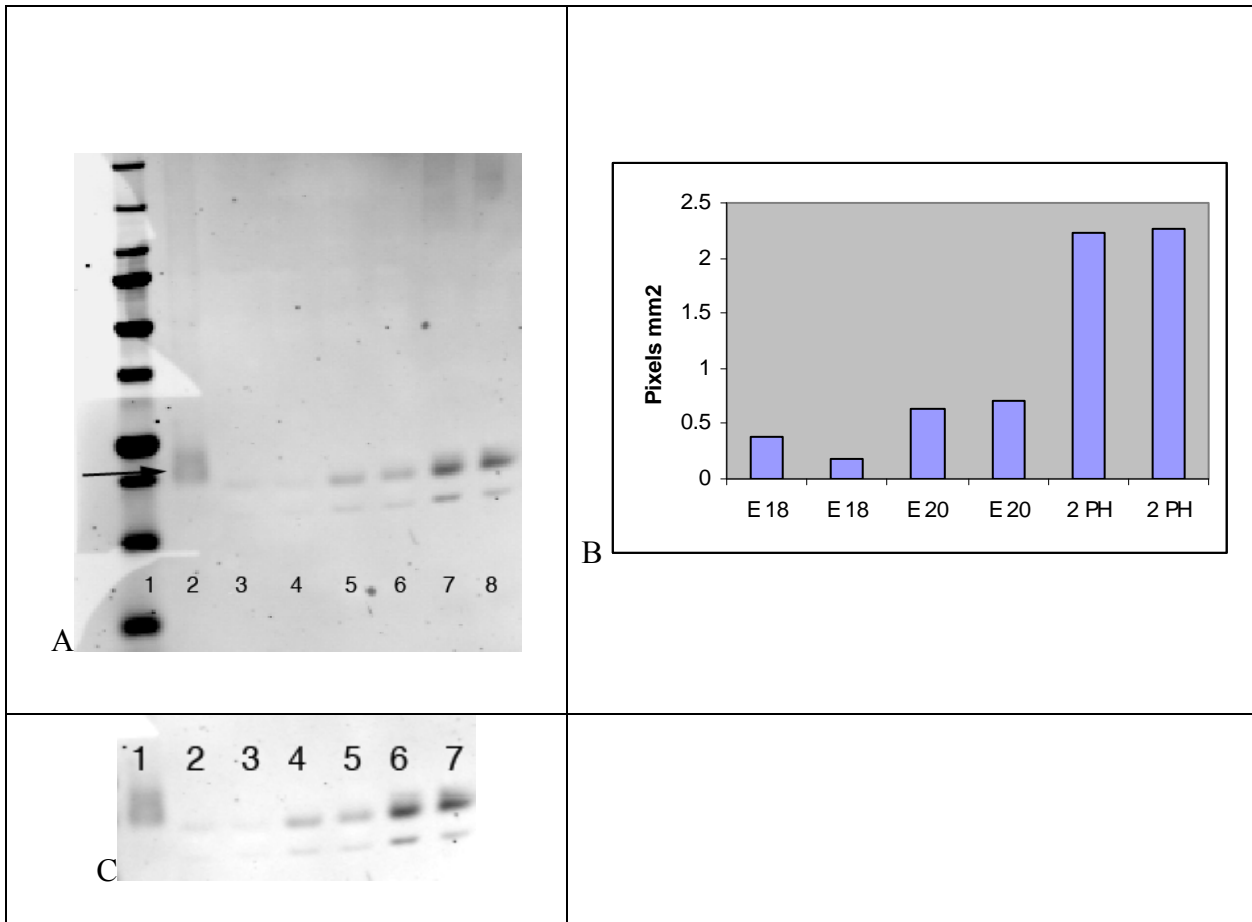


Figure 8. Claudin 2 expression in duodenal epithelium from pre- and post-hatch chicks

Figure A. Odyssey scan of claudin 2 immunoblot. Lanes are loaded as follows: Lane 1) Molecular weight marker, Lane 2) 30ug rat kidney positive control, Lanes 3-4) 30ug 18-day duodenal epithelium, Lanes 5-6) 30ug 20-day duodenal epithelium, Lanes 7-8) 30ug 2-day post-hatch duodenal epithelium x 2. Figure B. Integrated intensity values from claudin 2 immunoblot expressed in pixels mm². Figure C. Crop of claudin 2 bands lanes 2-8.

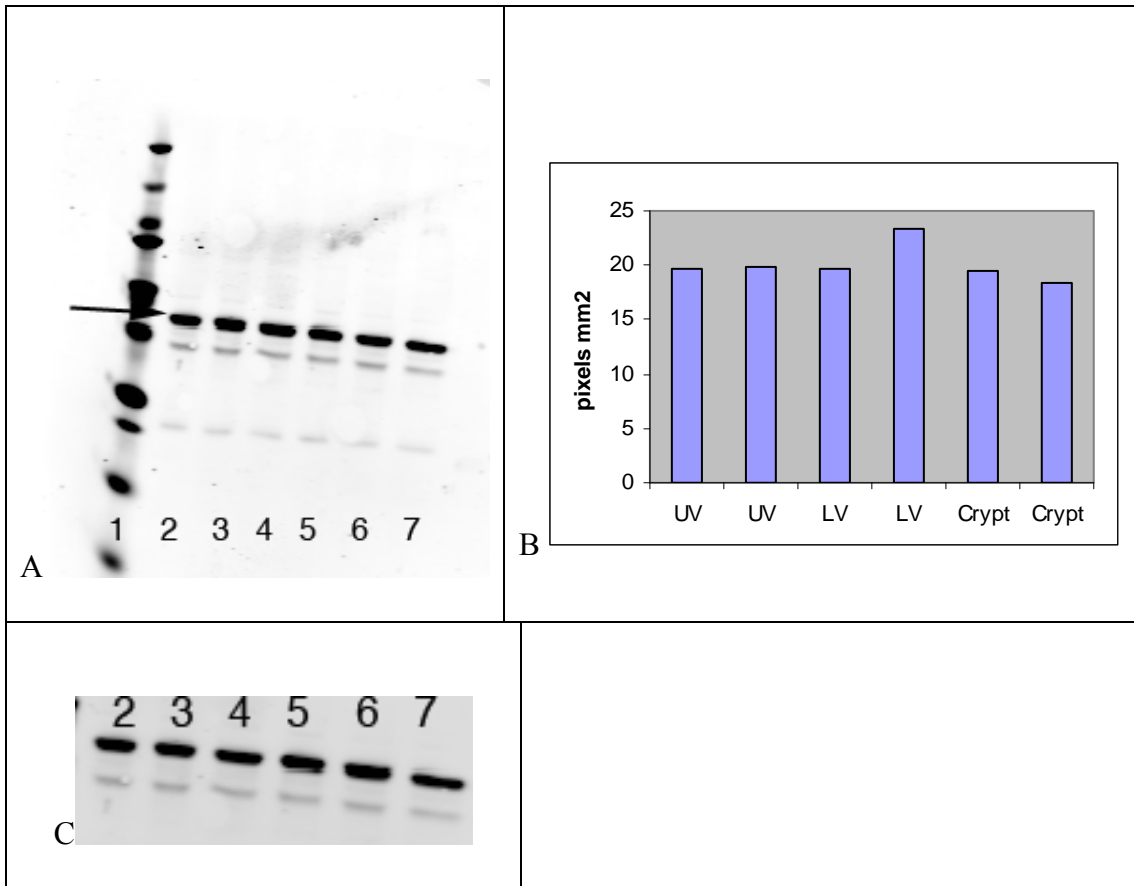


Figure 9. ERK 1 expression in duodenal epithelium along the crypt-villus axis of 2-day post-hatch chicks.

Figure A. Odyssey scan of ERK 1 immunoblot. Lanes are loaded as follows: Lane 1) Molecular weight marker, Lanes 2-3) 10ug cells from upper villus, Lanes 4-5) 10ug cells from lower villus, Lanes 6-7) 10ug cells from crypt (N=3). Figure B. Integrated intensity values from ERK 1 immunoblot expressed as pixels mm². Figure C. Crop of ERK 1 and 2 bands Lanes 2-7.

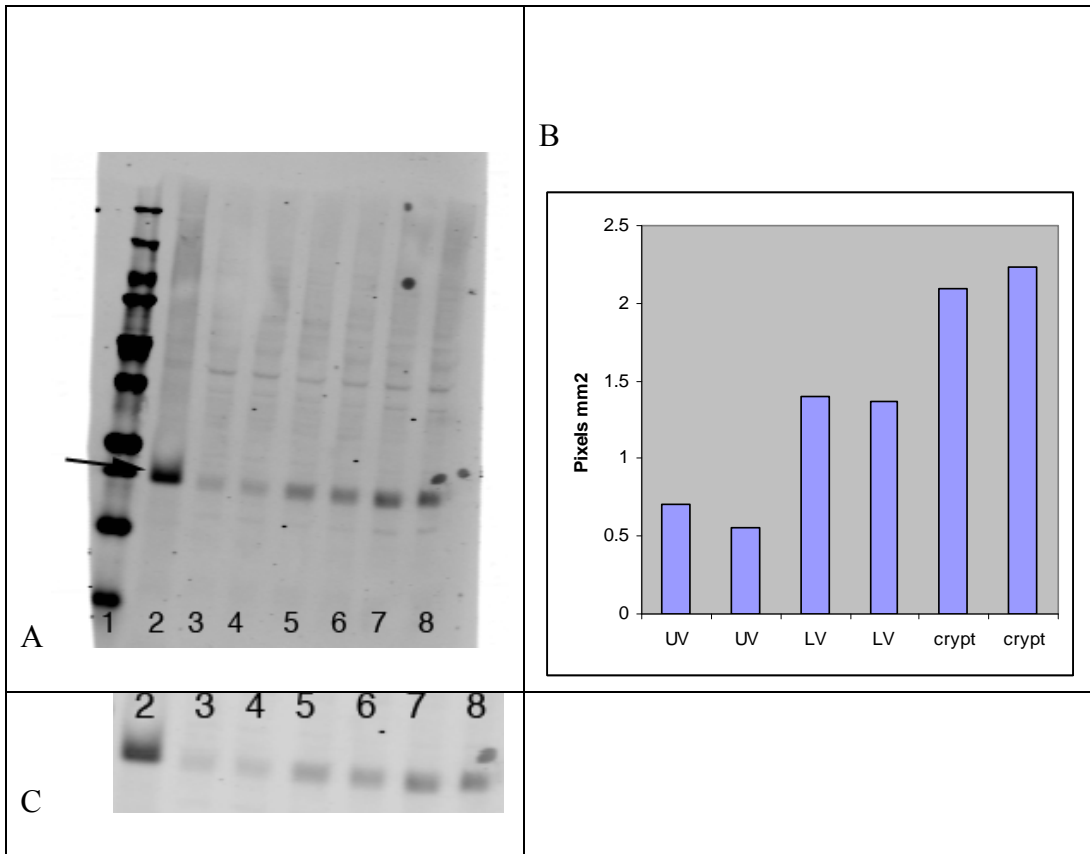


Figure 10. Claudin 2 expression in duodenal epithelium along the crypt-villus axis of the 2- day post-hatch chicks.

Figure A. Odyssey scan of Claudin 2 immunoblot. Lanes are loaded as follows: Lane 1) Molecular weight marker, Lane 2) 30ug rat kidney positive control, Lanes 3-4) 30ug cells from upper villus, Lanes 5-6) 30ug cells from lower villus, Lanes 7-8C 30ug cells from crypt (N=3). Figure B. Crop of Claudin 2 bands Lanes 2-8. Figure C. Integrated intensity values from Claudin 2 immunoblot expressed as pixels mm².

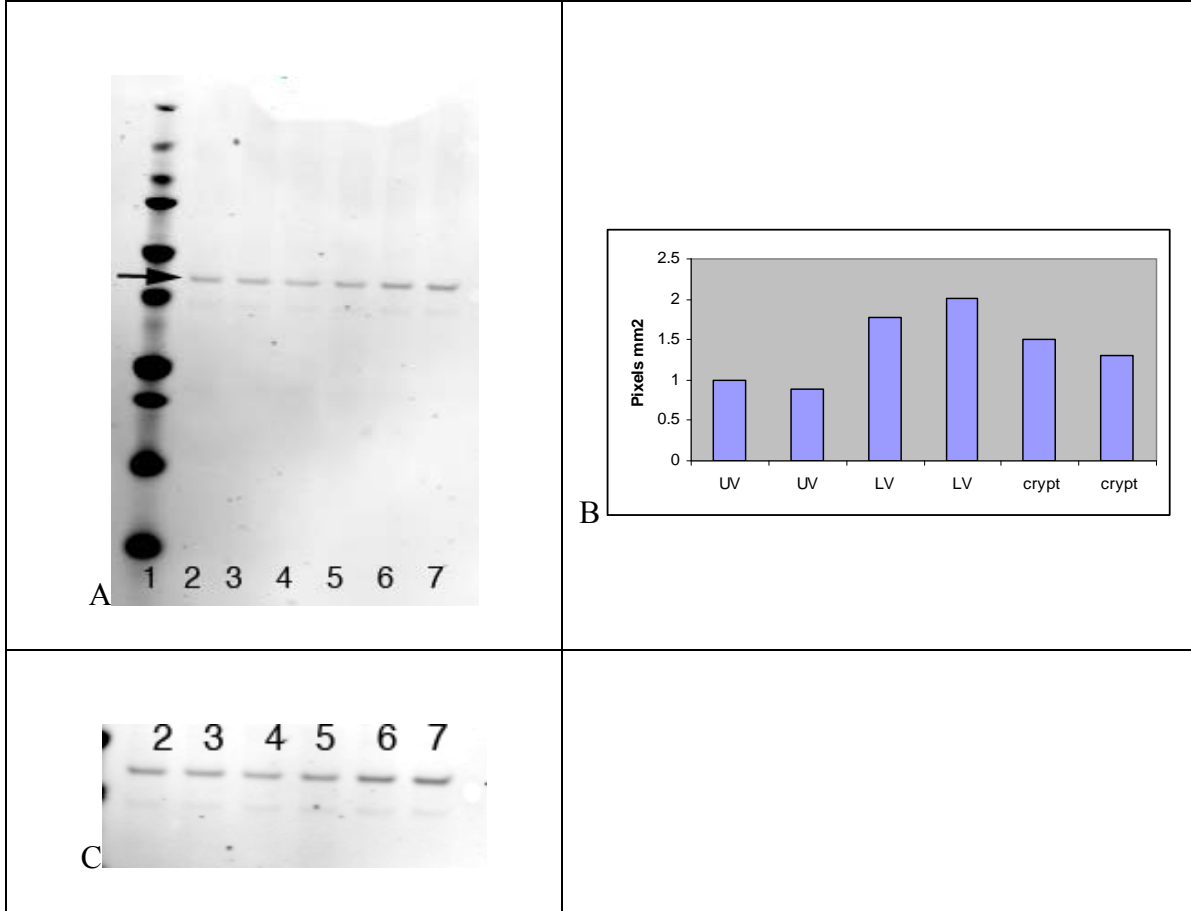


Figure 11. ERK 1 expression in duodenal epithelium along the crypt-villus axis of 20- day embryos.

- A. Odyssey scan of ERK 1 immunoblot. Lanes are loaded as follows: Lane 1) Molecular weight marker, Lanes 2-3) 10ug cells from upper villus, Lanes 4-5) 10ug cells from lower villus, Lanes 6-7) 10ug cells from crypt (N=3). Figure B. Integrated intensity values from ERK 1 immunoblot expressed as pixels mm². Figure C. Crop of ERK 1 bands Lanes 2-7.

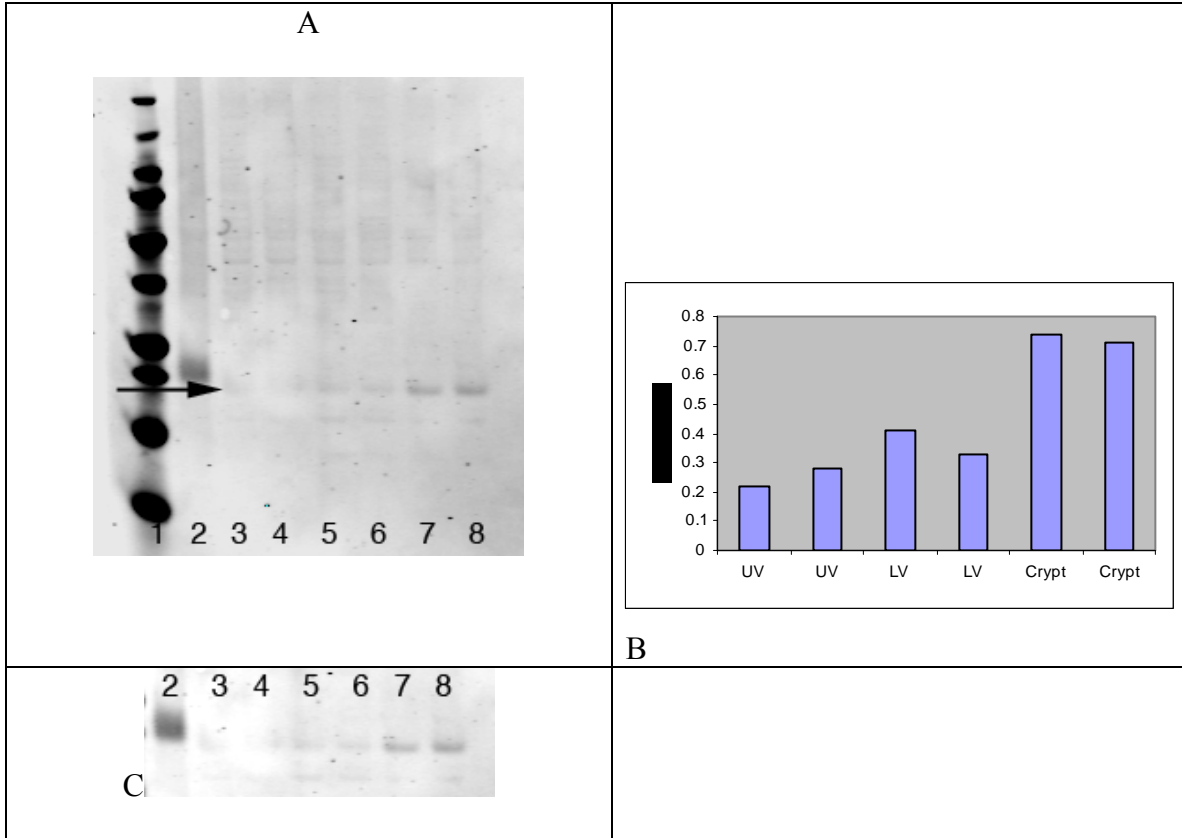


Figure 12. Claudin 2 expression in duodenal epithelium along the crypt-villus axis of 20-day embryos.

Figure A. Odyssey scan of Claudin 2 immunoblot. Lanes are loaded as follows: Lane 1) Molecular weight marker, Lane 2) 30ug rat kidney positive control, Lanes 3-4) 30ug cells from upper villus, Lanes 5-6) 30ug cells from lower villus, Lanes 7-8) 30ug cells from crypt X2 (N=3). Figure B. Integrated intensity values from claudin 2 immunoblot expressed as pixel mm². Figure C. Crop of Claudin 2 bands.

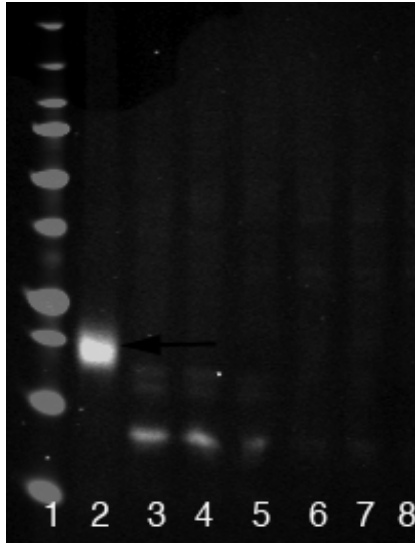


Figure 13. Claudin 4 expression in duodenal epithelium from pre- and post-hatch chicks.

Odyssey scan of claudin 4 immunoblot. Lanes are loaded as follows: Lane 1) Molecular weight marker, Lane 2) 5ug rat kidney, Lanes 3-4) 60ug 18-day duodenal epithelium, Lanes 5-6) 60ug 20-day duodenal epithelium, Lanes 7-8) 60ug 2-day post-hatch duodenal epithelium. Only kidney positive control lane has a clear band at 20Kda as indicated by the arrow.

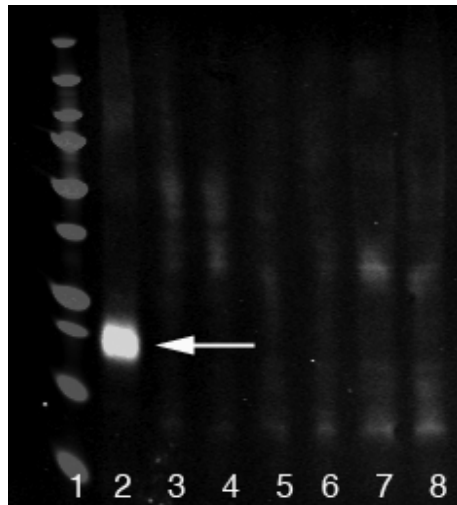


Figure 14. Claudin 4 expression in duodenal epithelium along the crypt-villus axis of 2-day chicks.

Odyssey scan of claudin 4 immunoblot. Lanes are loaded as follows: Lane 1) Molecular weight marker, Lane 2) 5ug rat kidney positive control, Lanes 3-4) 75ug cells from upper villus, Lanes 5-6) 75ug cells from lower villus, Lanes 7-8) 75ug cells from crypt (N=3). Note only Lane 2 containing the rat kidney positive control has the correct band for claudin 4 at 20 Kda (arrow).

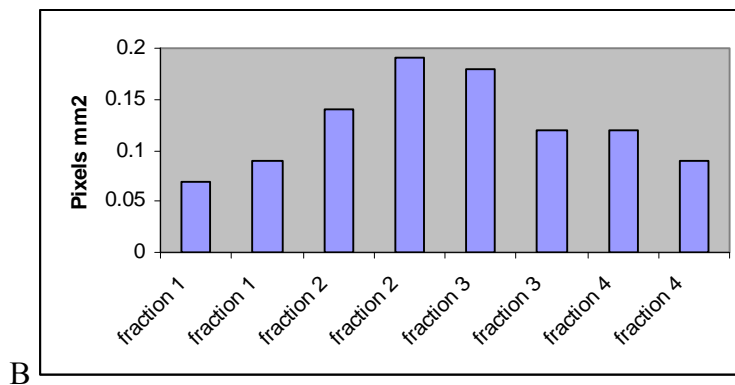
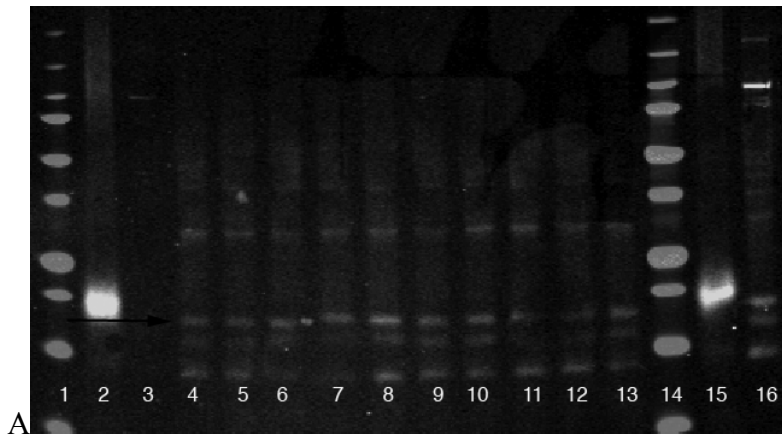


Figure 15. Claudin 4 expression in duodenal epithelium of a 3-week old chicken. Odyssey scan of claudin 4 immunoblot. Figure A. Lanes are loaded as follows: Lane 1) Molecular weight marker, Lane 2) 5ug rat kidney positive control, Lane 3) 5ug bird kidney, Lanes 4-5) 60ug cells from fraction 1, Lanes 6-7) 60ug cells from fraction 2, Lanes 8-9) 60ug cells from fraction 3, Lanes 10-11) 60 ug cells from fraction 4, Lanes 12-13) 60ug cells from fractions 1-4 combined whole villus and crypt, Lane 14) molecular weight marker, Lane 15) 5ug rat kidney positive control, Lane 16) 60ug bird kidney (N=1). Figure B. Integrated intensity values from claudin 4 immunoblot Lanes 4-11 expressed as pixel mm².

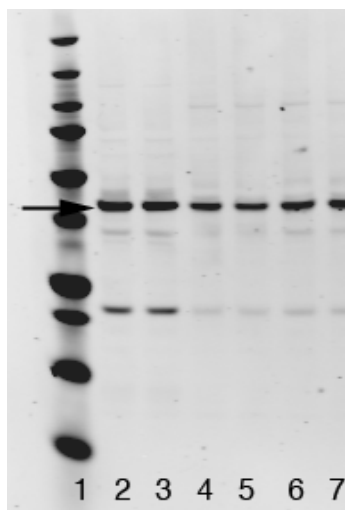


Figure 16. ERK 1 expression in duodenal epithelium from a 3-week old chicken. Odyssey scan of ERK 1 immunoblot. Lanes are loaded as follows: Lane 1) Molecular weight marker, Lanes 2-3) 10ug bird kidney, Lanes 4-5) 10ug cells from fraction, Lanes 6-7) 10ug cells from fraction 2 (N=1).

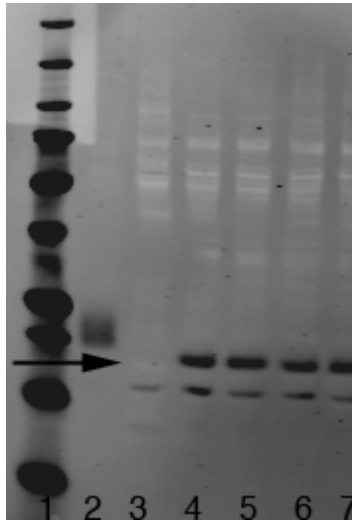


Figure 17. Claudin 2 expression in duodenal epithelium of a 3-week old chicken. Odyssey scan of claudin 2 immunoblot. Lanes are loaded as follows: Lane 1) Molecular weight marker, Lane 2) 30ug rat kidney positive control, Lane 3) 30ug bird kidney, Lanes 4-5) 30ug cells from fraction 1, Lanes 6-7) 30ug cells from fraction 2 (N=1).

Section V. Literature Cited

- Anderson, J. M. (2001). Molecular structure of the tight junction and their role in epithelial transport. News Physiol Sci. 16:126-130. Review.
- Anderson, J. M. and Van Itallie C. M. (2001). Tight junctions and the molecular basis for regulation of paracellular permeability. Am J Physiol. 269(4 Pt 1):G467-75. Review.
- Anderson, J. M. and Van Itallie C. M. (2006). Claudins and epithelial paracellular transport. Annu Rev Physiol. 68:403-29. Review.
- Andreeva, A.Y. Krause, E. Müller, E.C. Blasig, I.E. and Utepbergenov, D.I. (2001). Protein kinase C regulates the phosphorylation and cellular localization of occludin. J Biol Chem. 276(42):38480-6.
- Barker, N. van de Wetering, M. and Clevers, H. (2008). The intestinal stem cell. Genes Dev. 22(14):1856-64. Review.
- Black, B. L. (1976). Hormonal control of development in cultured embryonic chick intestine. Thesis. Washington University, St. Louis.
- Black, B. L. (1978) Morphological development of the epithelium of the embryonic chick intestine: Influence of thyroxine and hydrocortisone. Am J Anat. 153:573-600.
- Black B. L. (1998a). Development of glucose active transport in embryonic chick intestine. Influence of thyroxine and hydrocortisone. Comp Biochem Physiol. 90 A (3): 379-386.
- Black B. L. (1988b). Influence of hormones on glycogen and glucose metabolism in embryonic chick intestine. Am J Physiol. 254: G65-G73.

- Black, B. L. and Moog, F. (1977). Goblet cells in embryonic intestine: accelerated differentiation in culture. Science, New Series. 197: 368-370.
- Black, B. L. and Moog, F. (1978). Alkaline phosphatase and maltase in the embryonic chick intestine in culture. Developmental Biology. 66:232-249.
- Black, B. L. and Mack, C. M. (2002). Calcium distribution and modulation of goblet cell differentiation in embryonic intestinal epithelium. Molecular Biology of The Cell. 12: 2336. Suppl. S.
- Black, B. L. and Rogers, J. O. (1992). Development of calcium homeostasis in epithelial cells from embryonic and neonate intestine. Am J Physiol. 263. Gastronintest Liver Physiol. 26: G371-G379.
- Black, B. L. and Smith, J. E. (1989). Regulation of goblet cell differentiation by calcium in embryonic chick intestine. FASEB J. 3: 2653-2659.
- Brizuela, B.J. Wessely, O. De Robertis, E.M. (2001). Overexpression of the Xenopus tight-junction protein claudin causes randomization of the left-right body axis. Dev Biol. 230 (2): 217-29
- Burgess, D. R. (1975). Morphogenesis of intestinal villi. II. Mechanism of formation of previllous ridges. J Embryol Exp Morph. 34 (3): 723-740.
- Coulumbre, A. J. and Coulumbre, J. L. (1958). Intestinal Development. I. Morphogenesis of the villi and musculature. J Embryol Exp Morph. 6 (3): 403-411.
- Furuse, M. Fugita, K. Hiragi, T. Fugimoto, K. and Tsukita, S. (1998a). Claudin-1 and -2: novel integral membrane proteins localizing at tight junctions with no sequence similarity to occludin. J Cell Biol. 141(7):1539-50.

Furuse, M. Sasaki, H. Fugimoto, K. and Tsukita, S. (1998b). A single gene product, claudin-1 or -2, reconstitutes tight junction strands and recruits occludin in fibroblasts. J Cell Biol. 143(2):391-401.

Grimes, B. H. and Black, B. L.(1987). Morphological and metabolic differentiation of epithelium along the crypt-villus axis of chicken intestine. J Cell Biol. 105:195a.

Hamburger, V. and Hamilton, H. L. (1951). A series of normal stages in the development of the chick embryo. J Morphol. 88: 49-92.

Hauck, A.L. Swanson, K.S. Kenis, P.J. Leckband, D.E, Gaskins, H.R. and Schook, L.B. (2005). Twists and turns in the development and maintenance of the mammalian small intestine epithelium. Birth Defects Res C Embryo Today. 75(1):58-71. Review.

Hilton, W. A. (1902). The morphology and development of intestinal folds and villi in vertebrates. Am J Anat. 1: 459-504.

Hinni, J. B. and Watterson, R. L. (1963). Modified development of the duodenum of chick embryos hyposectomized by partial decapitation. J Morph. 113: 381-462.

Holmes, J.L. Van Itallie, C.M. Rasmussen, J.E. and Anderson, J.M. (2006). Claudin profiling in the mouse during postnatal intestinal development and along the gastrointestinal tract reveals complex expression patterns. Gene Expr Patterns. (6):581-8.

Hou, J. Gomes, A.S. Paul, D.L. and Goodenough D.A. (2006). Study of claudin function by RNA interference. J Biol Chem. 281(47):36117-2.

Kimura, M. Sawada, N. Kimura, H. Isomura, H. Hirata, K. and Mori, M. (1996). Comparison between the distribution of 7H6 tight junction-associated antigen and occludin during the development of chick intestine. Cell Struct Funct. 21(1):91-6.

Krause, G. Winkler, L. Mueller, S.L. Haseloff, R.F. Piontek, J. and Blasig IE. Structure and function of claudins. (2008). Biochim Biophys Acta. 1778(3):631-45.

Ma, T.Y. Tran, D. Hoa, N. Nguyen, D. Merryfield, M. and Tarnawski, A. (2000). Mechanism of extracellular calcium regulation of intestinal epithelial tight junction permeability: role of cytoskeletal involvement. Microsc Res Tech. 51(2):156-68.

Mankertz, J. Hillenbrand, B. Tavalali, S. Huber, O. Fromm, M. and Schulzke, J.D. Functional crosstalk between Wnt signaling and Cdx-related transcriptional activation in the regulation of the claudin-2 promoter activity. Biochem Biophys Res Commun. 314(4):1001-7.

Marandi, S. De Keyser, N. Stilmant, C. Saliez, A. Sokal, E.M. Guiot, Y. and Buts, J.P. (2002). Ontogeny of MAP kinases in rat small intestine: premature stimulation by insulin of BBM hydrolases is regulated by ERKs but not by p-38 MAP kinase. Pediatr Res. 52(2):180-8.

Mariadason, J.M. Nicholas, C. L'Italien, K.E. Zhuang, M. Smartt, H.J. Heerdt, B.G. Yang, W. Corner, GA. Wilson, AJ. Klampfer, L. Arango, D. and Augenlicht, L.H. (2005). Gene expression profiling of intestinal epithelial cell maturation along the crypt-villus axis. Gastroenterology. 128(4):1081-8.

Marcial, M.A. Carlson, S.L. and Madara, J.L. (1984). Partitioning of paracellular conductance along the ileal crypt-villus axis: a hypothesis based on structural analysis with detailed consideration of tight junction structure-function relationships. J Membr Biol. 80(1):59-70.

Moog, F. (1950). The functional differentiation of the small intestine. I The accumulation of alkaline phosphomooesterase in duodenum of the chick. J Exp Zool. 115: 019-129.

Moog, F. and Thomas, E. R. (1957). Functional differentiation of small intestine. VI. Transient accumulation of glycogen in the intestinal epithelium of chick embryo under normal conditions and under influence of hydrocortisone. Physiol Zool. 30: 281-287.

Morita, K. Furuse, M. Fujimoto, K. and Tsukita, S. (1999). Claudin multigene family encoding four-transmembrane domain protein components of tight junction strands. Proc. Natl Acad Sci USA. 96(2):511-6.

Ozden, O. Black, B. L. and Brizuela, B. J. Developmental profile of Claudin-3, Claudin-5, and Claudin 16 tight junction proteins in the chick intestine. (2004). ETD. etd-10282004-132349.

Pinto, D. and Clevers, H. (2005). Wnt control of stem cells and differentiation in the intestinal epithelium. Exp Cell Res. 306(2):357-63. Review.

Rahner, C. Mitic, L.L. and Anderson, J.M. (2001). Heterogeneity in expression and subcellular localization of claudins 2, 3, 4, and 5 in the rat liver, pancreas, and gut. Gastroenterolgy. 120(2):411-22.

Raya, A. Kawakami, Y. Rodriguez-Esteban, C. Ibañes, M. Rasskin-Gutman, D. Rodrigues-León, J. Büscher, D. Feijó, J. A. and Belmonte, J. C. (2004). Notch activity acts as a sensor for extracellular calcium during vertebrate left-right determination. Nature. 427: 121-128.

Rogers, J. O. and Black, B. L. (1996). The effect of hydrocortisone and thyroxine on development of calcium homeostasis in embryonic intestinal epithelium. Experimentia. 52: 558-563.

Saitou, M. Fugimoto, K. Doi, Y. Itoh, M. Fugimoto, T. Furuse, M. Takano, H. Noda, T. and Tsukita, S. (1998). Occludin-deficient embryonic stem cells can differentiate into polarized epithelial cells bearing tight junctions. J Cell Biol. 141(2):397-408.

Sakaguchi, T. Gu, X. Golden, H.M. Suh, E. Rhoads, D.B. and Reinecker, H.C. (2002). Cloning of the human claudin-2 5'-flanking region revealed a TATA-less promoter with conserved binding sites in mouse and human for caudal-related homeodomain proteins and hepatocyte nuclear factor-1 alpha. J Biol Chem. 277(24):21361-70.

Schröder, N. and Gossler, A. (2002). Expression of Notch Pathway components in fetal and adult mouse small intestine. Gene Expression Patterns 2. 247-250.

Scoville, D.H. Sato, T. He, X.C. and Li L. (2008). Current view: intestinal stem cells and signaling. Gastroenterology. 134(3):849-64. Review.

Simon, D.B. Lu, Y. Choate, K.A. Velazquez, H. Al-Sabban, E. Praga, M. Casari, G. Bettinelli, A. Colussi, G. Rodriguez-Soriano, J. McCredie, D. Milford, D. Sanjad, S. and Lifton, R.P. (1999). Paracellin-1, a renal tight junction protein required for paracellular Mg²⁺ resorption. Science. 285(5424):103-6.

Sklan, D. Geyra, A. Tako, E. Gal-Gerber, O and Uni, Z. (2003). Ontogeny of brush border carbohydrate digestion and uptake in the chick. Br J Nutr. 89(6):747-53.

Tipsmark, C.K. Baltzegar, D.A. Ozden, O. Grubb, B.J. and Borski, R.J. (2008). Salinity regulates claudin mRNA and protein expression in the teleost gill. Am J Physiol Regul. Integr Comp Physiol. 294(3):R1004-14.

Tsukita, S. and Furuse M. (2000). The structure and function of claudins, cell adhesion molecules at the tight junction. Ann N. Y. Acad Sci. 915:129-35. Review.

Weber, S. Schneider, L. Peters, M. Misselwitz, J. Rönnefarth, G. Böswald, M. Bonzel, K.E. Seeman, T. Suláková, T. Kuwertz-Bröking, E. Gregoric, A. Palcoux, J.B. Tasic, V. Manz, F. Schärer, K. Seyberth, H.W. Konrad, M. (2001). Novel paracellin-1 mutations in 25 families with familial hypomagnesemia with hypercalciuria and nephrocalcinosis. J. Am Soc Nephrol. (9):1872-81.

Weiser, M.M. (1973). Intestinal epithelial cell surface membrane glycoprotein synthesis. I. An indicator of cellular differentiation. J Biol Chem. 248(7):2536-41.

Uni, Z. Geyra, A. Ben-Hur, H. and Sklan, D. (2000). Small intestinal development in the young chick: crypt formation and enterocyte proliferation and migration. Br Poult Sci. 41(5):544-51.